Review

Development, image interpretation, clinical experience, and applications of optical coherence tomography in neurointerventional surgery

Demetrius Lopes,[1] Ricardo A Hanel,[2] Vania Anagnostakou ,[3] Nicole M Cancelliere ,[4] Jens Fiehler,[5,6] Ivan Lylyk ,[7] Pedro N Lylyk,[7] Aymeric Rouchaud ,[8,9] Géraud Forestier ,[10,11] Adel M Malek ,[12] Kunal Vakharia ,[13] Maxim Mokin,[13] Christopher S Ogilvy ,[14] Eric Osborn,[15,16] Hiram Bezerra,[17] Shiro Uemura,[18] Adnan Siddiqui,[19] Tommy Andersson,[20,21] Matthew J Gounis ,[22] Pedro Lylyk,[7] Vitor M Pereira,[4] Giovanni J Ughi [23,24]

► Additional supplemental material is published online only. To view, please visit the journal online (https://doi.org/10.1136/jnis-2025-024359).

For numbered affiliations see end of article.

Correspondence to
Professor Giovanni J Ughi;
giovanni.ughi@protonmail.com

Received 4 December 2025
Accepted 31 January 2026
Published Online First
20 February 2026

Check for updates

© Author(s) (or their employer(s)) 2026. No commercial re-use. See rights and permissions. Published by BMJ Group.

To cite: Lopes D, Hanel RA, Anagnostakou V, *et al*. *J NeuroIntervent Surg* 2026;**18**:1796–1811.

ABSTRACT

Angiography remains the standard imaging modality for evaluating vascular disease and guiding endovascular interventions; however, its limited spatial resolution restricts visualization of vessel wall pathology and therapeutic devices. Over the past decade, intravascular optical coherence tomography (OCT) has emerged as a transformative tool in coronary artery disease. OCT provides three-dimensional, high-resolution imaging of coronary arteries, enabling assessment of vessel wall microstructure, plaque composition, lumen geometry, and stent deployment. This level of detail has advanced the understanding of coronary pathology and contributed to improved outcomes in percutaneous coronary interventions. Major cardiology societies now recommend the use of intravascular imaging, including OCT, for complex coronary interventions with level 1A evidence.

OCT is now expanding beyond the coronary vasculature, with growing interest in its potential role in neurointerventional surgery. While limited use of OCT has been reported in the neurovasculature, the characteristics of a coronary OCT device prevent routine use in intracranial arteries. A new generation of intravascular OCT technology has been developed for the tortuous and complex anatomy of cerebral vessels. Early clinical experience has investigated its safety, feasibility, and utility for intracranial vascular imaging. Neuro-dedicated OCT technology could represent a significant advancement in cerebrovascular imaging, offering insights beyond the capabilities of current modalities, with the potential to improve current understanding of neurovascular pathology and refine diagnostic and therapeutic strategies. Successful translation of OCT into neurointervention, however, also requires establishing principles for image interpretation to assess neurovascular disease and therapeutic devices. This article aims to provide guidance for interpreting OCT imaging of intracranial arteries. In addition, it reviews applications of OCT in neurointervention and describes the development of neuro-specific OCT technology.

INTRODUCTION

Neuroendovascular procedures rely on contrasted fluoroscopic imaging to guide device deployment and to ensure safety and effectiveness of the intervention. Although vessel angiography acquired with different imaging techniques provides excellent lumenograms and has long served as the gold standard for diagnosis of neurovascular disease, its inherent limitations (ie, a representation of the contrast-filled lumen and limited spatial resolution) fail to depict critical aspects of the vessel pathology and therapeutic devices. Current imaging modalities, such as digital subtraction angiography (DSA), CT angiography (CTA), cone-beam CTA, and magnetic resonance angiography (MRA) are limited by a spatial resolution >0.1 mm and are therefore unable to accurately characterize fine vessel-wall structures, underlying arterial wall pathology, device-vessel interactions, and the healing process of therapeutic devices. Catheter-based imaging modalities, including intravascular ultrasound (IVUS) and optical coherence tomography (OCT), have been used for vascular applications for decades. They have found routine clinical use in optimizing coronary interventions and have made significant contributions to advancing our understanding of atherosclerosis.[1 2] As ultrasound penetrates deep into lipid-rich plaques, IVUS offers a complete representation of the entire atherosclerotic coronary plaque burden and the external elastic lamina. On the other hand, OCT offers higher spatial resolution enabling detailed arterial disease characterization and accurate measurements of the arterial lumen dimensions. OCT also offers accurate visualization and characterization of thrombus, dissections, and therapeutic devices, resulting in images clearer and easier to interpret.[3 4]

In the last decade, OCT has become widely used in coronary interventions to complement angiographic guidance. By 2017, over 100 000 coronary OCT procedures were performed annually, with numbers steadily increasing.[5] Since the early 2010s, coronary OCT technology has also been explored for neurovascular applications. The high-resolution

J NeuroIntervent Surg: first published as 10.1136/jnis-2025-024359 on 20 February 2026. Downloaded from http://jnis.bmj.com/ on November 15, 2026 by guest. Protected by copyright, including for uses related to text and data mining, AI training, and similar technologies.

imaging characteristics of OCT have been recognized as an optimal intravascular imaging modality for the visualization of neurovascular disease and therapeutic devices, with the potential to enhance neurovascular treatment strategies, therapeutic device development, and understanding of cerebrovascular disease. Furthermore, the all-optical design of OCT catheters makes it suitable for miniaturization, offering opportunities for adaptation for use in intracranial arteries. However, as reported in previous publications by multiple groups,[6 7] the stiffness and dimensions of current OCT catheters designed for coronary use are unsuitable for navigation and imaging in tortuous cerebral vasculature. A novel OCT technology designed specifically for use in neurointervention has been recently introduced to address these limitations.[8 9]

In recent years, several articles have discussed the use of OCT in neurointerventional surgery to improve diagnosis, and reviews have summarized its applications for cerebrovascular diseases.[10 11] Most of these studies, however, also reported on carotid and extracranial arteries, whereas this article focuses on intracranial applications of OCT.

To provide sufficient context, we first introduce intravascular OCT technology and summarize the extensive evidence supporting OCT for cardiology applications. We then review studies using coronary OCT technology for intracranial imaging, reporting its limitations. Next, we review the development of neuro-specific OCT technology and introduce the fundamentals of image interpretation in intracranial arteries, providing a reference for future users.

INTRAVASCULAR OCT IMAGING TECHNOLOGY

The technical principles of intravascular OCT imaging have been reported by several previous articles.[12 13] As such, we have limited this section to summarizing fundamental aspects to facilitate improved understanding of the contents of this article and the basic principles of neurovascular OCT imaging. OCT technology is based on the detection of backscattered light from tissue. Similar to a radar, OCT illuminates its target with infrared light and measures the distance and intensity of the backscattered 'echoes' to generate a depth-resolved image. Light travels a distance of 10 µm (0.01 mm) in just ~30 femtoseconds (ie, 3×10^{-14} s), however, which exceeds the capabilities of today's fastest optical detectors to resolve. As such, OCT uses the principles of interferometry to determine from what depth light was reflected inside a sample. Modern intravascular OCT systems operate in the near-infrared range, typically using light sources with a central wavelength of 1300 nm and a bandwidth of ~70–100 nm. This choice of wavelength balances losses from tissue scattering and absorption to optimize imaging performance in vascular tissue. Intravascular OCT imaging provides an axial resolution in tissue of ~10–15 µm, making it particularly effective for high-resolution visualization of the vessel wall microstructure and therapeutic devices (eg, stents).

For catheter-based applications, near-infrared light is delivered to the artery inner wall via an optical fiber enclosed within a protective sheath. The catheter optics consists of an optical fiber terminated near the catheter tip, with a miniaturized focusing lens, polished at an angle for side-viewing. The optical lens illuminates the tissue and collects the backscattered light, which is transmitted through the fiber back to the console, where it is processed and analyzed. OCT images are generated and displayed in real time. Circular, two-dimensional, cross-sectional images are acquired by illuminating the artery while rotating and retracting the catheter inner optics. This results in a spiral sampling pattern, similar to conventional CT. Fine spacing (ie, ≤0.2 mm) of cross-sectional images results in a comprehensive volumetric imaging of the vessel.

CORONARY OCT IMAGING

Coronary imaging catheters are designed with a monorail (rapid exchange) tip for navigation over a guidewire. Recent technological advancements have enabled OCT catheters with crossing profiles under 2.0 F.[14 15] Navigation and accurate positioning of the catheter in coronary arteries is achieved under angiographic guidance using radiopaque markers. Because near-infrared light is attenuated by erythrocytes, OCT requires transient blood clearance to obtain interpretable images. This is accomplished using a brief injection of iodinated contrast media, which displaces blood from the imaging field while the system performs an automated pullback of the optical lens within the imaging catheter. Following image acquisition, modern systems can co-register OCT data with the angiogram, providing procedural reference in localizing and identifying specific anatomic regions, aiding decision-making.

The use of coronary OCT enables more accurate diagnostic assessment than angiography alone. OCT imaging provides accurate, quantitative, volumetric measurements of lumen dimensions and stenosis severity. Furthermore, by visualizing tissue optical properties (ie, scattering and absorption), OCT provides high-resolution imaging of plaque composition, identifying calcific, lipid, and fibrous components. OCT also enables visualization of fine arterial wall features, identifying conditions such as plaque rupture, thrombus, and dissections, and enables high-resolution visualization of coronary stents.

Routine clinical use is supported by structured workflows that facilitate image-guided intervention. These systematic approaches include baseline (ie, pre-intervention) OCT imaging for procedural planning and strategy selection, followed by postintervention imaging to confirm stenting results and to assess the need for further optimization.[16] By providing detailed characterization of atherosclerosis and quantification of luminal dimensions prior to intervention, OCT supports procedural planning and guides optimal vessel preparation. In predominantly lipid-rich or fibrotic lesions, direct stenting is often preferred, whereas in calcified lesions, plaque modification before stent deployment should be considered as poorly modified severe calcifications correlate with suboptimal stent expansion and increased risks of restenosis and thrombosis.[17] OCT also enables identification of optimal stent landing zones, informing device selection and sizing. Following stent deployment, OCT is performed to assess the device-pathology relationship, measure the minimal stent area, and quantify the degree of luminal expansion. Other issues, such as incomplete lesion coverage, severe stent strut malapposition, edge dissections, and excessive tissue protrusion can be readily identified, allowing the operator to address them intraprocedurally.

OCT is also used for guidance in percutaneous coronary intervention of lesions involving coronary-artery branch points. At bifurcation sites, precise stent placement is critical to avoid side-branch compromise. OCT helps by visualizing stent malapposition and underexpansion over the side-branch ostium, prompting additional balloon angioplasty to ensure that both the main and branch vessels are fully scaffolded and the stent well expanded.[18] In patients presenting with in-stent restenosis and stent thrombosis, OCT permits identification of the underlying restenosis mechanism, guiding appropriate treatment planning and therapy.[19]

J NeuroIntervent Surg: first published as 10.1136/jnis-2025-024359 on 20 February 2026. Downloaded from http://jnis.bmj.com/ on November 15, 2026 by guest. Protected by copyright, including for uses related to text and data mining, AI training, and similar technologies.

Safety of coronary OCT

A prospective registry showed that coronary OCT is safe in an unselected and heterogeneous group of patients with varying clinical settings.[20] This study monitored over 1000 procedures using OCT, finding that invasive imaging-related complications were rare (0.5%), self-limiting after retrieval of the imaging catheter or easily treatable in the catheterization laboratory, and reported no major adverse events, prolongation of hospital stay, or permanent patient harm. Although use of OCT may increase the contrast volume, trials have not observed higher rates of acute kidney injury.[21] Another study showed that, following predefined workflow with OCT guidance, fewer cineangiography views were needed compared with angiography guidance alone, leading to slightly decreased radiation exposure and with no difference in contrast utilization between groups.[22]

Coronary OCT randomized clinical trials and meta-analyses

Recent randomized controlled trials (RCTs)[21 23–25] along with recent meta-analyses encompassing more than 20 000 patients,[26 27] published in the last 5 years are summarized in online supplemental Table 1 (see Material and Methods section for the search methodology). These studies have demonstrated that incorporating OCT into clinical practice improves coronary intervention procedural results and, in selected patient populations, clinical outcomes. In 2025, following the most recent RCT publications, the American College of Cardiology and the American Heart Association Joint Committee released revised Clinical Practice Guidelines for the management of patients with acute coronary syndromes. A class I, level A recommendation was made stating that 'In patients with acute coronary syndromes undergoing coronary stent implantation in the left main artery or in complex lesions, intracoronary imaging with IVUS or OCT is recommended for procedural guidance to reduce ischemic events.'[28] Similarly, the European Society of Cardiology released revised guidelines in the second half of 2024. A class I, level A recommendation was made stating that 'Intracoronary imaging guidance by IVUS or OCT is recommended for performing percutaneous coronary intervention on anatomically complex lesions, in particular left main stem, true bifurcations, and long lesions.'[29] The Japanese Circulation Society and the Japanese Association of Cardiovascular Intervention and Therapeutics recommend the use of intravascular imaging, including OCT, to guide optimal percutaneous coronary intervention.[30]

EARLY INVESTIGATIONS USING CORONARY OCT TECHNOLOGY IN NEUROINTERVENTIONS

We present a narrative review on the use of coronary OCT technology in neurointervention. The methodology is reported in the Material and Methods section. The search was limited to reports using OCT in intracranial arteries, either in the anterior circulation or in the posterior circulation. This search identified 21 articles published between August 2011 and October 2025. These studies included 237 patients: posterior circulation arteries (n=220, 92.8%) and few selected anterior circulation arteries with limited tortuosity (n=17, 7.2%). Table 1 lists the

Table 1 Studies using coronary OCT devices for the evaluation of intracranial artery pathology. "N" is equal to the number of cases reported in the article.

Authors	N	Anatomy	Study
Patel et al (2013)[69]	1	Posterior	Case report, OCT imaging of V4 stenosis
Brouwer et al (2014)[70]	1	Posterior	Case report, OCT assessment of basilar dolichoectasia before and after flow-diverter treatment
Given et al (2014)[71]	1	Posterior	Case report, OCT imaging of V4 stent thrombosis
Griessenauer et al (2017)[72]	1	Anterior	Case report, OCT imaging of flow-diverting stent endothelialization
Gao et al (2018)[73]	1	Posterior	Case report, OCT imaging of spontaneous basilar artery dissection
Martínez-Galdámez (2018)[35]	1	Anterior	Case report, OCT imaging of a PCOM aneurysm treated with a flow-diverting stent
Pasarikovski et al (2019) 37[74]	3	Posterior	Case series, OCT imaging following basilar artery endovascular thrombectomy
Li et al (2020)[75]	1	Posterior	Case report, OCT imaging of V4 stenosis and disease characterization
Xu et al (2020)[76]	4	Posterior	Case series, OCT imaging of V4 stenoses >70% and disease characterization
Feng et al (2021)[77]	1	Posterior	Case report, OCT imaging of V4 in-stent restenosis
Feng et al (2021)[6]	49	Posterior	Original research, OCT imaging of V4 stenotic segments
Neira et al (2021) [78]	1	Anterior	Case report, OCT imaging of recanalized unruptured internal carotid artery Aneurysm previously treated with stent-assisted coiling
Yang et al (2021)[7]	33	Anterior (n=9) and posterior (n=24)	Original research, OCT feasibility for the imaging of intracranial atherosclerotic stenosis
Xu et al (2022) [31]	7	Posterior	Case series, initial OCT evaluation of macrocalcifications as a risk factor for in-stent restenosis
Li et al (2023)[79]	1	Anterior	Case report, OCT imaging of MCA filling defect after endovascular thrombectomy
Li et al (2023)[80]	1	Posterior	Case report, OCT imaging of residual basilar artery stenosis following endovascular thrombectomy
Li et al (2024)[32]	39	Posterior	Original research, OCT investigation of macrocalcifications as a risk factor for in-stent restenosis
Li et al (2024)[81]	1	Posterior	Case report, OCT imaging of basilar artery severe stenosis
Ma et al (2024)[82]	3	Posterior	Case series, OCT imaging in flow-diverting stent embolization of vertebral basilar artery dissecting aneurysms
Gutiérrez et al (2025) [34]	5	Anterior (n=4) and posterior (n=1)	Case series, OCT acute evaluation of flow-diverting stent characteristics for the treatment of intracranial aneurysms
Xu et al (2025)[33]	82	Posterior	Original research, OCT evaluation of V4 stenosed segments>70% and thrombosis

MCA, middle cerebral artery; PCOM, Posterior Communicating Artery.

J NeuroIntervent Surg: first published as 10.1136/jnis-2025-024359 on 20 February 2026. Downloaded from http://jnis.bmj.com/ on November 15, 2026 by guest. Protected by copyright, including for uses related to text and data mining, AI training, and similar technologies.

studies identified. In this section, we limit our review to original research studies and case series with five or more patients.

In 2021, Feng *et al* evaluated intracranial vertebral artery (V4) stenosis in patients (n=49) using coronary OCT technology.[6] The authors compared minimum diameter stenosis measured on DSA with OCT-derived minimum lumen area. Authors reported that OCT, owing to its higher resolution and true volumetric imaging, more accurately quantified the stenotic area, which may better predict clinical events. This study highlighted that OCT visualization of plaque characteristics provided information complementary to X-ray-based imaging (eg, size, composition, and other features, such as overlying thrombus), which may improve risk stratification. However, this experience also identified limitations of existing OCT catheters as coronary device stiffness is suboptimal for tortuous intracranial arteries and emphasized the need for an OCT solution specifically designed for the intracranial circulation.

Also, in 2021, Yang *et al* reported OCT usage to evaluate intracranial atherosclerotic disease (n=33 patients) with angiographically verified stenosis ≥70% undergoing treatment with balloon-mounted or self-expanding stents.[7] Lesions were mostly located in the posterior circulation (n=24) and in a limited number of selected anterior circulation cases (n=9). OCT imaging was successful in 81.8% of all cases, with failures due to poor image quality or inability to advance the catheter to the target segment owing to tortuosity. Further quantitative analysis for known OCT artifacts (eg, rotational distortions and axial discontinuities) showed that among 52 pullbacks, only 50% achieved 'grade 3' image quality (≥90% of cross-sections suitable for analysis). Vascular tortuosity predicted imaging success, highlighting inherent limitations of coronary devices for intracranial vessels. Nevertheless, when feasible, authors reported that the high resolution of OCT enabled assessment of plaque morphology and composition at a level unattainable with CTA, MRA, or DSA, including features associated with high-risk plaques (eg, neovascularization).

In a 2022 case series, Xu *et al* used OCT in a small series of patients with calcified intracranial vertebral artery stenosis (n=7), demonstrating accurate characterization of intracranial calcifications and reporting hypothesis-generating evidence that macrocalcifications may predict in-stent restenosis.[31]

Building on this work, in 2024, the same group (Li *et al*) reported the use of coronary OCT in 39 patients to evaluate the role of intracranial calcifications causing in-stent restenosis of vertebral arteries.[32] The presence of macrocalcifications within the stented segment (ie, fibrocalcific plaques with an arc >90 degrees) was associated with higher rates of restenosis, supporting the potential role of OCT to guide individualized treatment strategies in the future.

In 2025, Xu *et al* reported OCT imaging of native atherosclerotic plaques in the posterior circulation (intracranial vertebral or basilar artery) with stenosis >70% in 82 patients.[33] Cerebral infarction occurred more frequently in patients with in situ thrombus than in those without, indicating a higher risk in the thrombus group. OCT-derived area stenosis was found to be significantly greater in patients with thrombus and among patients presenting with lipid plaques. The presence of a thin fibrous cap was associated with more frequent in situ thrombus. Using OCT to characterize thrombus composition, a higher prevalence of fibrin-rich thrombi than erythrocyte-rich or mixed thrombi was found. These findings suggest the potential of OCT to more accurately detect non-occlusive thrombi overlying atherosclerotic plaques compared with conventional neurointerventional imaging methods, which may better inform treatment decision-making. Similar to the other studies, even in these less tortuous posterior circulation anatomies, the use of coronary OCT devices resulted in ~19% of cases being excluded owing to poor image quality.

In 2025, Gutiérrez-Baños *et al* used OCT in a case series of 5 patients to evaluate flow-diverting and other neurovascular stents used for brain aneurysm treatment.[34] Four patients underwent treatment in the anterior circulation (internal carotid artery) and one in the posterior circulation (basilar tip). OCT imaging was performed to assess acute procedural results and for follow-up examination. This initial experience indicated the potential role of OCT to complement DSA by depicting device-related issues (such as malapposition, in-stent thrombosis, or excessive endothelialization leading to stenosis) that can guide treatment. As in prior studies, authors reported that navigability of coronary OCT devices in neurovascular anatomy was challenging, emphasizing the need for devices dedicated to intracranial use.

NEUROSPECIFIC OCT TECHNOLOGY

Across early investigations using coronary OCT devices for neurointervention, usage has largely been restricted to posterior circulation intracranial arteries and, in a few cases, to selected anterior circulation arteries with minimal tortuosity proximal to the siphon of the internal carotid artery. In these reports, authors consistently highlighted the need for OCT systems specifically engineered for the intracranial circulation. Mechanical characteristics of coronary OCT catheters make them unsuitable for navigating the tortuous intracranial vasculature, and they cannot reliably provide artifact-free imaging under those conditions.[35] The unique features of intracranial arteries require different catheter-based OCT technology and an imaging console optimized for neurovascular use. Recognizing these limitations, early investigations used experimental prototypes to explore the initial feasibility of neurovascular OCT imaging in a very limited number of cases.[36 37]

More recently, a dedicated neuro-OCT imaging solution (*n*OCT™, Spryte Medical, Bedford, Massachusetts, USA) has been developed to address the requirements for imaging intracranial arteries. *n*OCT technology is currently available for investigational use only. The *n*OCT probe is miniaturized to achieve a profile comparable to that of standard neurovascular guidewires.[9] Like guidewires, it features a soft, atraumatic, radiopaque distal tip. The probe has an outer diameter of ~0.0165 inch and a flexible profile designed to safely navigate the severe bends encountered in the intracranial circulation. It can be delivered through neurovascular microcatheters and can image the entire 360° cross-section without the artifact generated by a guidewire. As in coronary imaging systems, the *n*OCT probe incorporates a rotating optical lens that focuses and collects near-infrared light backscattered from the vessel wall, neurovascular devices, and intraluminal structures. A single acquisition scans the vessel in approximately 2 s, providing high-resolution, three-dimensional imaging of the vessel wall microstructure and therapeutic devices. Unlike coronary systems, the entire *n*OCT probe is automatically retracted along the vessel during imaging, thus relinquishing distal access. No wire artifact is present. Similarly, the *n*OCT imaging console has also been optimized for neurovascular use. It provides a field of view of ~14.5 mm in diameter (larger than that of conventional coronary OCT systems), enabling visualization of arteries up to ~6–7 mm in diameter. It also offers a longer pullback, up to 100 mm. Together, the *n*OCT console and probe perform imaging at a high framerate, acquiring 250 cross-sectional images per second,

J NeuroIntervent Surg: first published as 10.1136/jnis-2025-024359 on 20 February 2026. Downloaded from http://jnis.bmj.com/ on November 15, 2026 by guest. Protected by copyright, including for uses related to text and data mining, AI training, and similar technologies.

resulting in dense, three-dimensional sampling along the vessel (cross-sectional spacing between ~0.10 mm and 0.15 mm, depending on acquisition settings), with an axial spatial resolution approaching 10 µm, which represents order(s) of magnitude improvement over DSA, CTA, and MRA.

Workflow integration

The *n*OCT probe integrates into existing neurovascular procedural workflows. The ~0.0165 inch profile enables navigation through microcatheters with an inner diameter of 0.021 inch or larger. The distal tip of the probe is radiopaque, enabling navigation under X-ray guidance. Once the probe is delivered to the target vascular segment, the microcatheter is retracted to unsheath it. Contrast is then delivered through the guide catheter or sheath, and, while continuously injecting contrast for a few seconds, the *n*OCT acquisition is triggered. The console automatically retracts the probe while acquiring 250 cross-sectional images per second, visualizing an arterial segment up to 100 mm in length in up to 2.7 s. During acquisition, images are displayed in real time. Once completed, the full imaging dataset is immediately available for review and analysis.

Initial preclinical and clinical experience with *n*OCT

The *n*OCT technology platform has been applied to several nonclinical in vivo models.[38–43] More recently, *n*OCT has been evaluated in a first-in-human experience involving 32 patients.[44] In this investigation, imaging encompassed 57 unique intracranial arteries from anterior (n=45) and posterior (n=12) circulations, investigating a wide range of disease states, including unruptured and ruptured intracranial aneurysms, intracranial stenoses, and vessel occlusions. Successful imaging was obtained in every patient, with artifact-free images independent of the radius of curvature (quantitative measure of tortuosity), showing feasibility in tortuous intracranial arteries. This initial clinical experience showed that routine volumes of contrast injection and blood clearance like the ones used for angiography (eg, 3DRA and CBCT) were suitable for *n*OCT imaging, resulting consistently in image quality in intracranial arteries despite the circle of Willis and collaterals present in the neurovascular anatomy.

OCT IMAGE INTERPRETATION IN NEUROVASCULAR DISEASE

OCT imaging interpretation has been extensively validated against gold-standard histopathology. Numerous histopathology studies have explored the use of OCT for assessing atherosclerotic plaques and coronary stents,[45–49] establishing the foundation for intravascular OCT image interpretation. These validation studies investigated the optical characteristics of vascular tissue and validated image interpretation of the normal vessel wall architecture as well as elements of vascular pathology, including, among others, the appearance of main plaque components (eg, fibrous, lipid, and fibrocalcific tissue), as well as the appearance of other vessel wall features (eg, plaque fibrous cap, and macrophages accumulation) and intraluminal objects (eg, thrombi).

It is important to note that interpreting OCT images, like any other medical imaging technique, involves prior anatomical knowledge coupled with an understanding of OCT image characteristics. This section reviews the basic principles of the physics of OCT image formation and provides guidance for the interpretation of images in the context of intracranial disease. Although OCT of intracranial arteries has a more limited evidence base compared with coronary applications, its use in evaluating neurovascular pathology has been explored in several in vivo and ex vivo studies,[37 40 50] as well as its ability to visualize the extravascular space surrounding intracranial arteries.[39 51] Building on existing knowledge and established criteria, this section aims to provide a framework for interpreting OCT imaging of the neurovasculature, drawing also on recent preclinical and clinical experience with *n*OCT.[8 9 39–44 52 53]

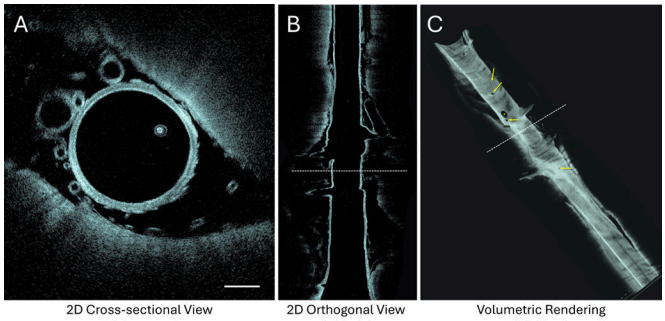


Figure 1 *n*OCT image visualization. (A) The image shows an example of *n*OCT cross-sectional (2D) imaging. (B) An example of a 2D *n*OCT orthogonal view. (C) An example of *n*OCT volumetric (3D) rendering. The dashed line on panels (B) and (C) indicates the location of the cross-sectional image presented in panel (A). Yellow arrows on image (C) indicate the location of small perforating arteries, whereas the asterisk shows the location of a larger branch. Scale bar=1 mm.

A final consideration is that the primary goal of this article is to outline the fundamentals of OCT image interpretation. Given the high-resolution capability of *n*OCT, which allows detection and quantification of tissue components analogous to histological features, it is not yet possible to anticipate all potential metrics and measurements that may prove relevant in intracranial artery assessment. Accordingly, the scope of this section is limited to basic measurements and interpretations. Future efforts will be needed to establish broader consensus and standardization for the analysis, interpretation, and reporting of neurovascular OCT imaging data as it relates to clinical manifestations. Likewise, as OCT remains in the early stages of clinical application in neurointervention, the significance of certain imaging findings will require further investigation.

Physical principles of OCT imaging for image interpretation

OCT uses *near-infrared light* to generate high-resolution cross-sectional images of intracranial arteries during contrast administration. Data are acquired at high speed (eg, 250 frames per second) and displayed as individual cross-sectional images (ie, frames). The imaging data are also presented as a two-dimensional orthogonal view of the acquisition (also known as longitudinal mode or L-mode) and different cut planes for the L-mode can be selected. Three-dimensional high-resolution renderings can also be generated. Figure 1 shows the different *n*OCT visualization methods.

The *refractive index* is a material property that affects the speed at which light propagates through a medium. When a light beam encounters a boundary between two tissues with different refractive indices (ie, optical impedances), part of the light is scattered, while the remainder is transmitted. OCT measures the intensity of the light that is reflected or backscattered by the tissue. The intensity of the OCT image, or the amount of backscattered light, is proportional to the refractive index difference between adjacent tissues. Image quality in OCT is primarily determined by contrast and spatial resolution. *Contrast* refers to the ability to distinguish backscattered light signals from background noise, while *spatial resolution* defines the minimum

J NeuroIntervent Surg: first published as 10.1136/jnis-2025-024359 on 20 February 2026. Downloaded from http://jnis.bmj.com/ on November 15, 2026 by guest. Protected by copyright, including for uses related to text and data mining, AI training, and similar technologies.

distance between two closely spaced structures that can be independently resolved. OCT systems are characterized by *sensitivity*, which indicates the minimum signal detectable above background noise, typically in the range of −100 dB (ie, achieving detection of less than 10^{-10} of the sample incident power) or better. The *dynamic range* is the difference between the minimal and maximal reflected signals that can be visualized, typically ranging from ~40 to 50 dB. In terms of spatial resolution, *n*OCT is defined in two directions: axial (parallel to the light beam) and lateral/transverse (perpendicular to the light beam). *Axial resolution* is determined by the spectral bandwidth of the laser light source, approaching ~10 microns. *Lateral resolution* is influenced by the light beam profile and probe optics. Miniaturized optics at the tip of the probe focus the light to a narrow spot, typically located ~2 mm away from the probe. Beyond this focal point, the beam diverges. The lateral resolution is optimal at the focal point, where the beam diameter is approximately 30 microns. The lateral resolution deteriorates with increasing distance from the focal point. *Penetration depth*, instead, refers to the extent to which OCT can provide useful imaging data from within tissue. As light travels through tissue, it undergoes attenuation due to scattering and absorption. At wavelengths of ~1300 nm, scattering is the dominant factor. The effective penetration depth of OCT through the arterial wall and surrounding tissue is primarily determined by the tissue composition. Highly attenuating tissues, such as lipid-rich regions and blood, limit the imaging depth, whereas tissues like collagen, fibrotic tissue, and calcium exhibit lower attenuation, allowing for deeper imaging. When imaging through cerebrospinal fluid and optically transparent media, OCT can visualize structures located several millimeters away from the artery.[39 54]

Tissue assessment

Normal vessel wall

OCT has sufficient resolution to visualize the individual layers of the arterial wall. The normal vessel wall typically exhibits a three-layered architecture, appearing in the images as: a thin, highly backscattering intima (ie, showing a bright appearance), a low-backscattering media (ie, appearing as a dark layer), and a highly backscattering adventitia (ie, showing a bright appearance) (figure 2). Given that the internal elastic lamina (IEL) has a thickness of <2 microns, OCT does not have sufficient resolution to visualize it directly, and the IEL is identified in OCT images as the boundary between the intima and media.

Extravascular space

The cerebrospinal fluid (CSF) is an optically transparent fluid enabling near-infrared light transmission and OCT imaging of the subarachnoid space surrounding intracranial arteries. Depending on the vessel's location, the arterial wall may be surrounded by CSF (figure 2A) or by periadventitial tissue (figure 2B). When CSF is present, the surrounding extravascular space and structures can be seen. Large surrounding arteries and small perforating arteries within the CSF appear as well-defined circular structures with a signal-poor inner lumen, whereas veins appear as circular structures with a signal-rich (ie, blood) inner lumen, followed by an optical shadow (figure 2A). In the subarachnoid space, arachnoid membranes and trabeculae appear as thin, high-backscattering, linear structures. Nerve roots appear as larger structures showing high backscattering and are recognized in the context of their anatomical location.[39] The brain parenchyma, dura mater, and bony structures appear as larger surrounding structures defining the visible CSF space. Among

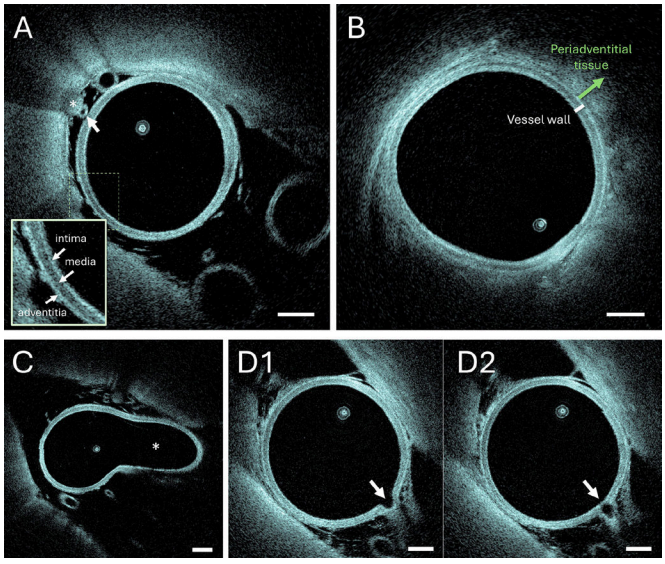


Figure 2 Normal arterial wall, side branches, and perforating arteries. (A) *n*OCT imaging in the middle cerebral artery (MCA) shows a normal, three-layered vessel wall architecture (inset) comprising a high-backscattering (bright) thin intima, a lower backscattering (darker) media, and a thin, high-backscattering adventitia. Cerebrospinal fluid, which surrounds the artery, is optically transparent, allowing visualization of extravascular structures. Small perforating arteries (arrow) appear as well-defined circular structures with signal-poor lumens filled with contrast, whereas veins (asterisk) appear as signal-rich structures containing blood, casting shadows that obscure underlying tissues. (B) *n*OCT cross-section from the cavernous segment of the internal carotid artery (ICA) shows a normal arterial wall (white line) surrounded by high-backscattering, signal-attenuating periadventitial tissue (green arrow). (C) The image shows the ICA bifurcation into the arterial cerebral artery (ACA) and MCA. The asterisk indicates the lumen of the ACA. (D1-D2) Two adjacent *n*OCT frames, showing the origin of a perforating branch of the basilar artery (arrow). Scale bars=1 mm.

others, the ability of OCT to image the extravascular space can be used to identify the transition between the intradural and extradural segments of the internal carotid artery (ICA). The visualization of tissue microstructure can also aid in the characterization of periadventitial tissue characteristics. The presence of erythrocytes in the CSF changes its appearance from transparent to opaque (erythrocytes strongly scatter near-infrared light), enabling assessment of the presence of blood (eg, occult or sentinel hemorrhage).[55]

Arterial lumen and side branches

OCT clearly defines the interface between the luminal border and the arterial wall, accurately depicting the three-dimensional lumen anatomy. The lumen contour can be automatically traced by the *n*OCT console and accurate measurements can be derived, including lumen area and lumen diameter (also including maximum and minimum lumen diameter and eccentricity). At branching points, OCT visualizes the arterial lumen of the main vessel, side branches (figure 2C), and small perforating branches (figure 2D), including their ostia.

Lumen stenosis and atherosclerotic plaques

Atherosclerotic plaques are typically characterized by a focal thickening of the arterial wall and by the loss of the normal layered vessel architecture. OCT can accurately measure

J NeuroIntervent Surg: first published as 10.1136/jnis-2025-024359 on 20 February 2026. Downloaded from http://jnis.bmj.com/ on November 15, 2026 by guest. Protected by copyright, including for uses related to text and data mining, AI training, and similar technologies.

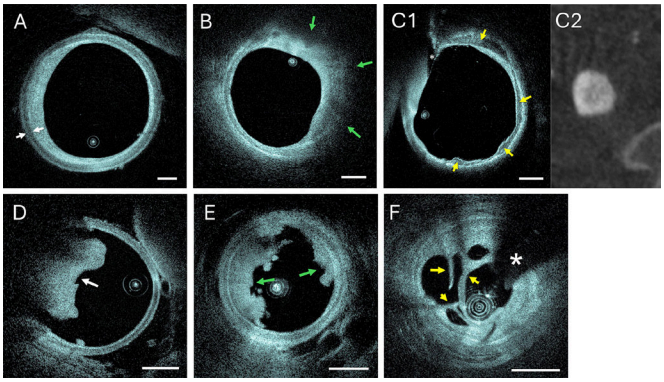


Figure 3 Intracranial atherosclerotic plaques and thrombus. (A) Fibrous plaque in the V4, with the media layer clearly visible (white arrows). (B) Eccentric lipid-rich plaque in the cavernous segment of the internal cerebral artery (ICA), appearing as a signal-poor region with poorly defined borders and a relatively thick fibrous cap spanning two quadrants circumferentially (green arrows). (C1) Fibrocalcific plaque in the ophthalmic segment of the ICA, demonstrating circumferential calcium deposition across three quadrants (yellow arrows). Calcium appears as a signal-poor region with sharply delineated borders. Variable calcium thickness is observed: a thin sheet in the lower quadrant and a slightly thicker fibrocalcific deposit in the upper quadrant. (C2) Corresponding high-resolution, contrast-enhanced cone-beam CT (VasOCT) image from approximately the same ICA location as the *n*OCT image. The lumen appears regular and, due to limited spatial resolution, the thin ring of subintimal calcium deposits is not visualized. (D) The white arrow indicates an erythrocyte-rich thrombus within the middle cerebral artery (MCA), characterized by high backscattering, strong optical attenuation, and a shadowing effect that obscures the underlying tissue. The arterial wall shows a normal appearance. (E) The green arrows identify a fibrin and platelet-rich thrombus adherent to the MCA wall, displaying homogeneous backscattering and low optical attenuation. The vessel wall beneath the thrombus demonstrates a normal three-layered architecture. (F) Example of a recanalized thrombus (in a coronary artery) exhibiting a honeycomb-like appearance with multiple channels. The yellow arrows highlight fibrous tissue layers separating these channels. Panel (F) is courtesy of Dr Timothy D Henry, The Christ Hospital, Ohio, USA. This image was acquired using a coronary imaging catheter (Gentuity LLC, Sudbury, MA). Scale bars=1 mm.

lumen stenosis severity, assess atherosclerotic plaque composition, and other morphological characteristics. OCT provides measurements of vessel minimum lumen area (MLA), as well as minimum diameter. The lumen area stenosis (%) can be derived by comparing the MLA to a reference (normal) segment of the vessel. As described in more detail below, OCT can distinguish between fibrous, lipid, and fibrocalcific plaques and provide measurements, including quantification of the plaque circumferential extension, the size of the media (ie, media to media diameter across the center of the lumen), and the thickness of the fibrotic cap overlying lipid and calcific plaques.

Atherosclerotic plaque components

1. *Fibrous plaques and intimal thickening*. Fibrous tissue appears as high-backscattering, relatively homogeneous regions with low optical attenuation (figure 3A). The media layer is often visible beneath the plaque. These plaques typically contain collagen and smooth muscle cells. OCT can accurately characterize their size and thickness.[56]
2. *Lipid plaques*. Histopathologic correlation studies using OCT define a *lipid plaque* as either having a necrotic core or a region within pathological intimal thickening that contains extracellular lipids or proteoglycans.[47] Lipid plaques appear as signal-poor areas with poorly defined borders (figure 3B). They are characterized by a rapid drop-off in OCT signal, with only their luminal surface being visible in the image. An overlying fibrous cap, visible as a high-backscattering, homogeneous layer, is often seen. OCT can assess the thickness of the cap and identify lipid plaques with a thin fibrous cap. Owing to the high optical attenuation caused by lipid plaques and necrotic cores, OCT is usually not capable of visualizing the full thickness and extent of large lipid-rich areas.
3. *Fibrocalcific Plaques*. On OCT, calcium appears as a signal-poor, heterogeneous region with sharply delineated borders and low optical attenuation (figure 3C). Fibrocalcific plaques contain a mixture of fibrous tissue and calcium. In intracranial arteries, calcium deposits vary in form, size, and shape and are typically categorized as micro- or macro-calcifications.[32] OCT allows precise assessment of the thickness of fibrous tissue overlying calcium, as well as quantification of the calcium area (circumferential extent) and thickness (superficial or deep calcifications). After plaque modification with balloon angioplasty or other techniques, the high resolution of OCT enables visualization of calcium fractures, providing a means to evaluate procedural effectiveness.
4. *Mixed plaques*. Because atherosclerosis is a progressive disease, plaques often present a heterogeneous (mixed) appearance, and individual OCT cross-sectional images may display features of multiple plaque types within the same lesion.

Thrombus

Thrombi typically appear on OCT as masses within the arterial lumen, either free floating or adherent to the vessel wall. They can be occlusive or non-occlusive. OCT is highly sensitive to the high attenuation of erythrocytes, which exhibit high backscattering and strong signal attenuation, thus it can delineate an erythrocyte-rich ('red') (figure 3D) versus an erythrocyte-poor ('white') thrombus composed of platelets, dense fibrin, and organized material that show a more homogeneous texture with lower backscattering and attenuation (figure 3E). It is important to note that most thrombi display mixed characteristics, with different regions showing different composition and features. A recanalized thrombus may appear as a honeycomb-like structure characterized by multiple intraluminal channels separated by thin fibrous tissue layers (figure 3F). These channels represent the pathways formed by partial restoration of blood flow through an organized thrombus. This distinctive appearance helps differentiate a recanalized thrombus from other intraluminal structures, such as plaque ruptures or dissections.

Ruptured or eroded plaques

Ruptured plaques typically occur in lipid-rich lesions with a thin fibrous cap. Acute plaque rupture is characterized by the presence of overlying erythrocyte-rich thrombus, a cavity in the arterial wall, and evidence of tearing, disruption, or dissection of the fibrous cap exposing the plaque content. Acute plaque erosion typically presents erythrocyte-poor thrombi and an irregular luminal surface but lacks evidence of cap rupture or cavity formation across consecutive OCT frames. One of the key differences between plaque rupture and erosion is that eroded plaques present an intact fibrous cap, with thrombosis caused by an eroded luminal surface (ie, lacking endothelial cells),[57] while

J NeuroIntervent Surg: first published as 10.1136/jnis-2025-024359 on 20 February 2026. Downloaded from http://jnis.bmj.com/ on November 15, 2026 by guest. Protected by copyright, including for uses related to text and data mining, AI training, and similar technologies.

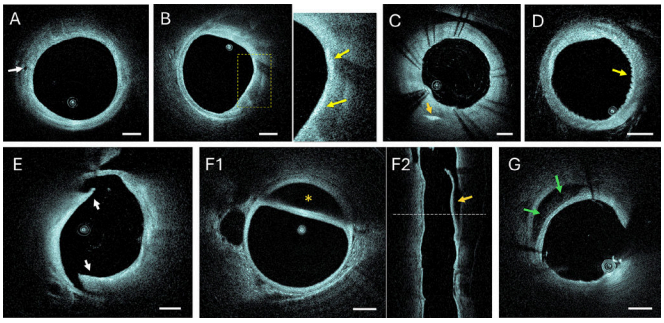


Figure 4 OCT Imaging of neovessels, macrophage accumulations, cholesterol crystals, vasospasm, dissections, and intramural hematoma. (A) *n*OCT image showing an intimal microvessel (white arrow). Intimal vessels appear as well-defined circular or oval structures with a central signal-poor lumen. (B) *n*OCT image showing macrophage accumulations in the fibrous cap of a lipid plaque in the cavernous segment of the internal carotid artery (ICA). Macrophage accumulations appear as focal, highly backscattering regions with shadowing behind them (inset, yellow arrow). (C) A cholesterol crystal is visible (orange arrow) in a previously stented V4 segment, appearing as a linear, highly backscattering structure embedded within the plaque. (D) *n*OCT imaging of vasospasm showing undulated internal elastic lamina and a concentric increase in media thickness and brightness, possibly due to smooth muscle cell contraction (yellow arrow). (E) *n*OCT image depicting an iatrogenic dissection following balloon angioplasty in the V4. Superficial tears within a concentric lipid plaque are visible (white arrows). (F1) *n*OCT imaging of an arterial dissection in an in vivo leporine model (the image is courtesy of Dr Romain Chauvet, CHU Limoges, France). The orange asterisk indicates the false lumen. (F2) *n*OCT horizontal projection aids in identifying the false lumen (orange arrow). The dashed line indicates the location of the cross-sectional image in F1. (G) Intramural hematoma (in a coronary artery) resulting from stent deployment (green arrow), appearing as a crescent-shaped, signal-poor (dark) region with sharply delineated inner borders. Panel (C) is adapted from *Sci Transl Med*. 2024 May 15;16(747):eadl4497 and reproduced with permission. Panel (G) is courtesy of Dr Harry M. Cohen, Advocate Heart Institute, Illinois, USA; this image was acquired using a coronary imaging catheter (Gentuity LLC, Sudbury, MA). Scale bars=1 mm.

ruptured plaques present with a ruptured cap, with thrombosis caused by exposing the content of the plaque. By assessing clot characteristics and the state of the fibrous cap, OCT enables the in vivo diagnosis of plaque erosion versus plaque rupture.[58]

Calcific nodules

Calcific nodules are superficial calcium deposits that protrude into the vessel lumen and may contribute to plaque instability. In coronary arteries, two histological types have been described. The first consists of dense calcium protrusions covered by a smooth, intact fibrous cap. The second, known as eruptive calcific nodules, is characterized by small, dense calcium fragments or nodules associated with fibrous cap disruption and overlying luminal thrombus,[59] often producing shadowing of the underlying plaque. Although calcific nodules have been identified in coronary OCT studies, their prevalence and characteristics within intracranial arteries remain to be clarified through future investigations.

Other plaque features

Neovessels (plaque vasculature) within the intima may be seen as small, signal-poor, well-defined circular structures (figure 4A). They are often identifiable across consecutive OCT frames in the presence of atherosclerosis. The presence of such microvasculature typically indicates an advanced stage of plaque development and higher risk of hemorrhage.[60] Lipid plaques may also contain accumulations of *macrophages*, which are known markers of plaque inflammation. Macrophage accumulations appear as high-intensity, signal-rich, punctate regions (figure 4B). Owing to their light-scattering properties, they can cast shadows that obscure deeper structures. *Cholesterol crystals* appear as thin, linear, high-intensity structures, often located within the fibrous cap of a lipid-rich plaque (figure 4C), and are also known to be associated with plaque instability.

Vasospasm

Vasospasm may result in luminal narrowing. On OCT, vasospasms can be recognized by characteristic morphological features, such as the presence of an intact three-layered architecture, undulated appearance of the IEL, and increased concentric thickness and brightness of the media, possibly from contraction of smooth muscle cells and by the absence of structural abnormalities, such as atherosclerotic plaques, thrombi, or dissections (figure 4D).

Dissections

Dissections appear as a tissue flap arising from the arterial wall (figure 4E,F). OCT can assess the extent of the dissection and classify it as intimal (confined to the intima or plaque cap) or transmural, extending into the media or adventitia. Various severity metrics have been proposed, based on circumferential extent, depth of penetration into the arterial wall, longitudinal length, and size of the residual lumen. Assessing consecutive *n*OCT cross-sectional images and the two-dimensional L-mode can assist in identifying the false lumen.

Intraplaque hemorrhage

Intraplaque hemorrhage is one of the pathophysiological processes that lead to atherosclerotic plaque progression and rupture. It has been linked to active bleeding from neovessels into the plaque. Intraplaque hemorrhage often appears as a signal-poor region within the plaque with limited optical attenuation (degenerated erythrocytes) and better delineated borders than lipid plaques. Fresh hemorrhage, however, can exhibit a higher optical attenuation due to the presence of intact erythrocytes.[61]

Intramural hematoma

Intramural hematomas present a crescent-shaped, low-signal (dark), area with sharply defined inner borders. They are typically related to the presence of dissections or focal intimal disruption overlying fibrous or lipid plaques and often occur secondary to balloon inflation or stent placement. Intramural hematomas usually present a cavity close to the lumen, showing a double-lumen appearance, with an intimal membrane separating the two lumens (figure 4G). The intramural hematoma can be visible in its entirety if of limited size, whereas the full extent might not be visible for those hematomas that are larger. Sometimes partial organization or thrombosis inside the hematoma can be seen.

Intracranial aneurysms

Aneurysms appear as structures arising from the parent artery (figure 5). OCT offers direct visualization of both the aneurysm neck and dome, if the size of the dome does not exceed its field of view. Tissue characteristics and composition of the aneurysm dome and neck can be seen, including disruption of the IEL and

J NeuroIntervent Surg: first published as 10.1136/jnis-2025-024359 on 20 February 2026. Downloaded from http://jnis.bmj.com/ on November 15, 2026 by guest. Protected by copyright, including for uses related to text and data mining, AI training, and similar technologies.

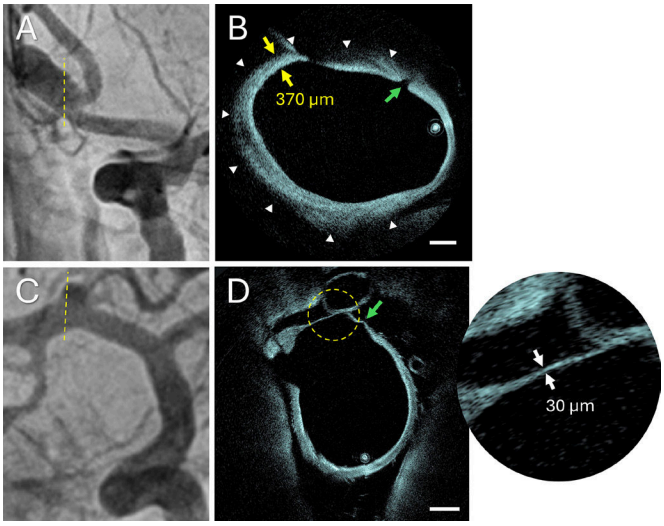


Figure 5 Intracranial aneurysms. (A) Angiography shows an anterior communicating artery aneurysm. The dashed line shows the approximate location of the *n*OCT cross-sectional image. (B) *n*OCT imaging reveals detailed morphology of the aneurysm. The dome appears as a circular structure arising from the parent artery (white arrowheads). It shows a thickened wall with a minimum tissue thickness of 0.37 mm (yellow arrows) and loss of the normal three-layered arterial structure. The luminal surface appears smooth, with no evidence of intraluminal thrombus. The surrounding cerebrospinal fluid (CSF) appears optically transparent, consistent with an unruptured aneurysm. A small perforating artery (green arrow) is visible near the aneurysm neck. (C) Angiography of a small lenticulostriate artery aneurysm. The dashed line shows the location of the *n*OCT cross-sectional image. (D) Corresponding *n*OCT imaging demonstrates a thin, hypocellular dome with a minimum thickness of 0.03 mm (inset, white arrows) and neck irregularities (green arrow). The transparent appearance of the CSF confirms an unruptured aneurysm. Panels (C) and (D) are adapted from *Sci Transl Med*. 2024 May 15;16(747):eadl4497, with permission. Scale bars=1 mm.

loss of a three-layered wall architecture, pathological thickening, presence of calcifications, macrophage accumulations, and presence of adherent thrombus. The neck's shape and size, as well as the minimum thickness of the dome tissue, can also be evaluated. OCT further enables visualization of the aneurysm's interaction with surrounding extravascular structures. Additionally, pathology of the parent artery extending from the aneurysm neck can be assessed.

Therapeutic device assessment

Intracranial stents and flow diverters

Metallic structures, such stents and flow-diverter struts, are opaque to light. As a result, only the leading (nearest) surface of metallic struts is visible on OCT, while a shadow is cast behind them, obscuring underlying structures (figure 6A).

Coils and intrasaccular devices

Like metallic stent struts, coils are opaque to light and appear as bright reflecting structures with shadowing behind them (figure 6B). Intrasaccular devices also appear as bright reflecting structures with shadowing behind them, with struts and other features (eg, detachment points) visible on OCT (figure 6C).

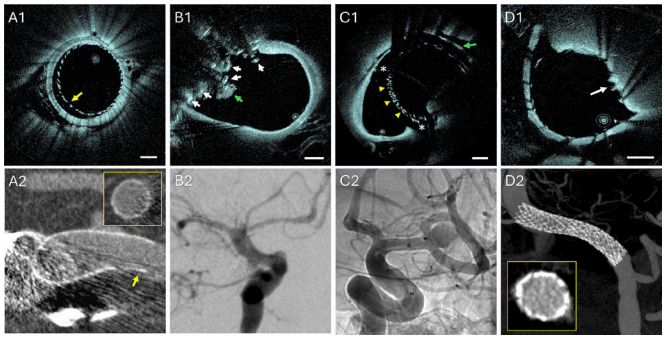


Figure 6 Imaging of therapeutic devices at baseline. (A1) *n*OCT imaging of a flow-diverting stent. Stent struts appear opaque to light, with only their luminal surface visible, followed by a narrow optical shadow. The yellow arrow indicates an area of malapposition, where the struts are separated from the vessel wall (maximum distance~0.27 mm). (A2) Corresponding contrast-enhanced cone-beam CT (CBCT) in the frontal oblique projection shows potential malapposition towards the distal end of the stent (yellow arrow), which is partially obscured by artifacts from the coil mass. Cross-section of the same region (inset) does not show the malapposed area. (B1) *n*OCT imaging of an aneurysm treated with multiple coils. White arrows identify the coils, which, being metallic, are opaque to light and cast shadows that obscure deeper structures. The green arrow highlights thrombus formation on top of the coil surface. (B2) Corresponding subtracted real-time fluoroscopy in the frontal projection taken at the same time as the *n*OCT imaging shows comparable findings with the coil mass within the aneurysm and preservation of the posterior communicating artery. Appreciation of early clot formation is not possible. (C1) *n*OCT imaging of an intrasaccular device. Arrowheads mark the device surface, with asterisks indicating gaps in aneurysm neck coverage. The green arrow delineates the aneurysm dome behind the device. (C2) Unsubtracted angiogram in a frontal oblique projection shows the intrasaccular device prior to detachment with apposition of the device at the level of the neck of the aneurysm and preservation of both middle cerebral artery branches. (D1) *n*OCT imaging of a large, eccentric lipid plaque treated with an intracranial, self-expandable, stent. The white arrow indicates plaque tissue protrusion between the stent struts. (D2) High-resolution contrast-enhanced CBCT in a frontal projection (VasOCT) shows a well-positioned stent covering the lesion and no signs of underexpansion or plaque protrusion. The cross-section of the vessel (inset) lacks the spatial or contrast resolution to demonstrate plaque components protruding between the stent struts. Scale bars=1 mm.

Device apposition

OCT enables precise measurements of deployed stents and flow-diverting stents' cross-sectional area, as well as their minimum and maximum diameters, and apposition to the arterial wall.[52 53] Malapposition is defined as a gap between the stent and the arterial wall that exceeds the thickness of the stent struts. Communicating malapposition is a malapposition involving the aneurysm neck (eg, endoleak).[53] The clinical significance of neuroendovascular device malapposition measured by OCT (eg, severity and location) merits further investigation. OCT can also be used to assess gaps in aneurysm neck coverage by coils and intrasaccular devices.[40 62]

Device, thrombus formation, and dissection

OCT can also visualize the presence of thrombus over the surface of therapeutic devices. In addition, OCT can accurately depict iatrogenic dissections (such as ones located at stent edges or following balloon angioplasty) and identify the true lumen of the artery.

J NeuroIntervent Surg: first published as 10.1136/jnis-2025-024359 on 20 February 2026. Downloaded from http://jnis.bmj.com/ on November 15, 2026 by guest. Protected by copyright, including for uses related to text and data mining, AI training, and similar technologies.

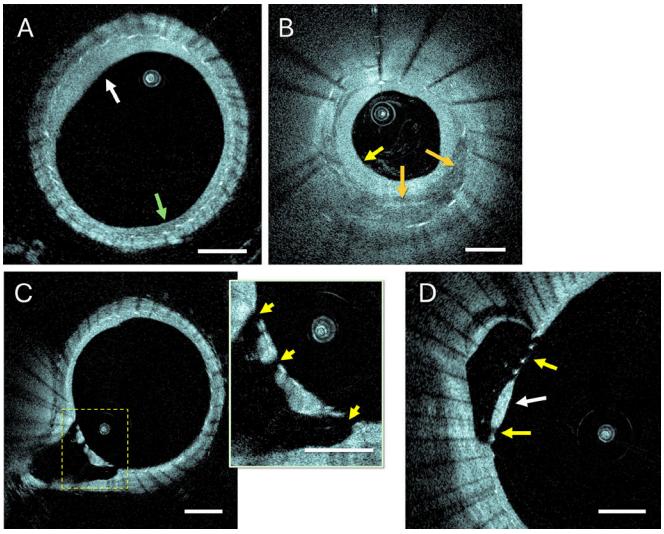


Figure 7 Therapeutic device follow-up imaging. (A) *n*OCT imaging demonstrates neointimal coverage over a flow-diverting stent. White and green arrows indicate neointimal tissue of varying thickness. (B) *n*OCT imaging of in-stent restenosis reveals a layered tissue structure, with a superficial, high-backscattering layer (yellow arrow) suggestive of smooth muscle cell proliferation, overlying deeper, low-signal tissue surrounding the stent struts (orange arrows). The luminal surface appears smooth and free of thrombus. (C) *n*OCT imaging of a stent-covered side branch at follow-up shows tissue coverage over the ostium, with multiple open channels visible (inset, yellow arrows). (D) *n*OCT imaging of an aneurysm neck remnant at follow-up reveals tissue growth across the flow-diverter struts (white arrow), while small residual channels remain patent within the neck remnant (yellow arrows). Scale bars=1 mm.

Plaque protrusion

Plaque protrusion appears as irregular or dome-shaped tissue, in continuation with the underlying plaque, protruding between stent struts into the stent lumen (figure 6D). It represents displaced or protruding plaque material that bulges into the lumen after stenting, sometimes due to compression of soft components, such as lipid plaque or thrombus. Its severity and extent in the lumen (eg, height) can be measured and quantified.

Neointimal coverage

Owing to its high-resolution imaging and the ability to visualize metallic devices without significant artifacts, OCT is an ideal modality for evaluating the vessel response to device implantation. The presence and characteristics of neointimal tissue growth over therapeutic devices can be accurately obtained at follow-up examinations (figure 7A). Struts are classified as *covered* if tissue is visible above them and *uncovered* if no tissue is present. Additionally, OCT provides insights into the type of neointimal tissue covering the struts, such as smooth muscle cells, extracellular lipids, and fibrin depositions.[49] The extent of neointimal response to flow diverters has been validated against classic histomorphometric analysis.[42]

Restenosis

OCT enables precise quantification of restenosis severity, including measurement of the residual lumen cross-sectional area. It can evaluate stent dimensions to detect and quantify stent underexpansion or malapposition, identify thrombus or uncovered struts, and plaque residuals at the stent edges. In addition, OCT provides detailed assessment of restenotic tissue morphology (figure 7B) and can differentiate between fibrotic hyperplasia, neoatherosclerosis, and other potential contributors, such as vasospasm, allowing accurate characterization of the underlying mechanism of restenosis.

Side-branch patency and aneurysm residual filling

By providing high-resolution visualization of side-branch ostia, OCT allows detailed assessment of side-branch patency after stent (or flow-diverting stent) deployment. It can identify obstructions of the side branch origin caused by stent struts or plaque shift (snowplow effect), which is caused by main vessel stenting, resulting in side-branch narrowing or occlusion. It can identify the presence of thrombus and tissue growth over the struts (figure 7C). Similarly, at follow-up examination, OCT visualizes aneurysm coverage gaps by tissue and devices, enabling the precise assessment of residual aneurysm neck fillings (figure 7D).

OCT artifacts

Recognizing artifacts is essential for accurate interpretation of OCT images. In this section, we review the most common artifacts. Image quality can be influenced by both the effectiveness of blood clearance and the presence of optical artifacts. Because many artifacts depend on the position of the OCT probe within the vessel lumen, it is important that readers always identify the probe's location when interpreting OCT images. Furthermore, correct interpretation of OCT imaging often relies on the careful review of adjacent cross-sections to distinguish artifact from true findings.

Incomplete vessel flushing and suboptimal blood clearance

Because erythrocytes attenuate near-infrared light, blood must be displaced from the arterial lumen (typically through a brief injection of contrast media). If blood is not completely cleared and mixes with the contrast, it can generate various artifacts or patterns in the images (figure 8A–C). Care should be taken when interpreting images with residual blood, as it can obscure the OCT signal and, in some cases, mimic the appearance of thrombus.

Optical reflections

As the light beam exits and re-enters the probe optics, it may reflect between different material interfaces within the probe, producing circular line artifacts in the image (figure 8D). Due to their characteristic circular appearance, these artifacts are usually easy to recognize and should not be mistaken for real tissue structures.

Axial saturation

When a highly reflective surface is oriented perpendicular to the probe, the intensity of the backscattered light may exceed the intensity range of the OCT system (figure 8E). This results in an artifact that appears as high-intensity lines radiating from the probe along the axial direction. Metallic therapeutic devices are common sources of such strong backscattering.

Orientation artifact

When the probe is in an eccentric position and lies close to a therapeutic device, the struts of a stent, flow diverter, or coil may appear to face the catheter from all directions (figure 8F). This phenomenon is often referred to as the 'sunflower' or 'merry-go-round' artifact.

J NeuroIntervent Surg: first published as 10.1136/jnis-2025-024359 on 20 February 2026. Downloaded from http://jnis.bmj.com/ on November 15, 2026 by guest. Protected by copyright, including for uses related to text and data mining, AI training, and similar technologies.

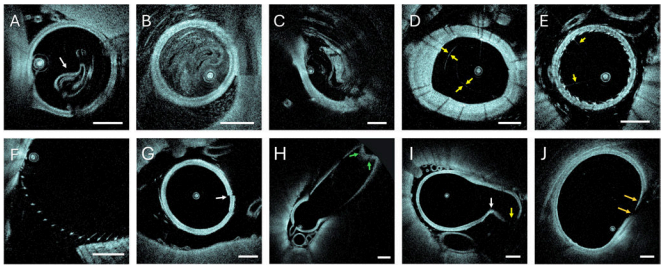


Figure 8 OCT imaging artifacts. (A) Example of suboptimal flushing and blood residuals. A limited amount of blood residual is seen in the lumen (white arrow), obscuring small portions of the tissue behind it. (B) Blood mixed with contrast with the arterial wall still visible. (C) Blood obscuring a large portion (>180 degrees) of the arterial wall. (D) Circular optical reflection artifacts (arrows) visible in the lumen. (E) Saturation artifacts extending along the axial direction. (F) Stent strut orientation artifact. Flow diverter struts appear oriented towards the probe location. (G) The white arrow shows a small axial discontinuity. (H) The green arrows point to a foldover artifact appearing when imaging a side branch. (I) The yellow arrow indicates a tissue-shadowing artifact. The light beam propagating from the probe is blocked by the ostial tissue (white arrow) obscuring a portion of the side-branch wall. (J) The orange arrows indicate a tangential signal drop-off artifact. When interpreting OCT images, the reader should always carefully consider the location of the imaging probe within the arterial lumen. Scale bars=1 mm.

Axial image discontinuity

If the probe moves relative to the vessel during the acquisition of a single cross-sectional image, an axial discontinuity may appear, resulting in misalignment of the image (figure 8G). Likewise, if variations in pullback speed significantly increase the longitudinal spacing within a single probe optics revolution, a similar axial discontinuity in the image may be observed.

Fold-over artifact

When the vessel diameter exceeds the OCT field of view, tissues or devices located beyond the imaging range may fold back and appear superimposed in the image, producing a fold-over artifact (figure 8H). Regions of the image affected by this artifact should be interpreted with caution.

Shadowing artifact

The light beam is attenuated as it passes through objects, such as thick tissue or metallic surfaces. Objects in the light beam path can create shadows that appear as drops in signal intensity and may diminish the image intensity of structures behind them, creating apparent discontinuities in the vessel wall (figure 8I).

Tangential dropout

When the probe is positioned close to the vessel wall, the light beam may strike the tissue surface at a shallow, nearly parallel angle. This artifact is more likely to occur when the probe is pressed against a flat or elevated region of the arterial wall. Like shadowing artifacts, the amount of backscattered light returning to the probe is reduced, leading to apparent discontinuities in the vessel wall (figure 8J). In some cases, as the light travels tangentially along the luminal surface, it can produce apparent signal attenuation that mimics the appearance of lipid-rich plaque or other attenuating structures. Therefore, caution should be exercised when interpreting tissue composition, and the probe's position should always be considered.

Vessel curvature

When the imaging probe is not aligned with the vessel's longitudinal axis (for example, in large tortuous vessels), the resulting image may appear elliptically distorted, reducing the accuracy of lumen measurements.

APPLICATIONS OF OCT FOR NEUROVASCULAR DISEASE

This section reviews the potential future use of neuro-dedicated OCT devices in the diagnosis and treatment of neurovascular disease, with a focus on ischemic and hemorrhagic stroke. While further clinical studies are needed to define the clinical role of OCT in neurointervention, the following sections outline potential applications based on the current evidence.

OCT applications in hemorrhagic stroke

By offering a high-resolution 'view from within', OCT imaging of intracranial aneurysms complements the lumen assessment obtained with DSA, CTA, and MRA, while revealing structural details that are otherwise unattainable. The near-histological resolution of OCT allows detailed evaluation of the aneurysm dome tissue, neck, and parent artery, as well as the presence of thrombus, providing insight into tissue pathology that extends beyond conventional parameters, such as patient demographics, aneurysm size, shape, and location. Histological studies have shown that dome wall thinning and disruption of the normal three-layered architecture as well as the cellular components of the dome and neck, together with other tissue characteristics such as dome shape (eg, presence of an irregular neck), may help assess aneurysm stability and identify lesions at higher risk of rupture.[63–65] The opaque appearance of the cerebrospinal fluid (ie, indicating the presence of erythrocytes) may identify aneurysm rupture status (in the case of subarachnoid hemorrhage with multiple aneurysms) or sentinel bleeding. The characteristics of the perivascular environment (eg, aneurysm location and interaction with surrounding structures) may further inform aneurysm vulnerability to rupture.[66]

During interventions, the detailed anatomical information provided by OCT for the aneurysm neck can guide device selection (eg, choosing between coiling, stent-assisted coiling, or flow diversion) to ensure optimal neck coverage and promote complete aneurysm occlusion. Likewise, high-resolution assessment of the parent artery can inform device choice and placement—for example, by helping to avoid deployment over perforating arteries or superficial calcifications that may delay healing[31] when unnecessary. Histological analyses have shown that after endovascular intervention, adequate wall apposition is strongly associated with complete aneurysm occlusion following flow-diverter therapy, whereas DSA or cone-beam CTA only provides limited accuracy for identifying malapposition.[67] OCT imaging enables precise assessment of acute stent or flow-diverter malapposition (its severity, extent, and location), including involvement of the aneurysm neck (eg, communicating malapposition, a known predictor of delayed occlusion), as well as adjacent branches and perforating arteries. By accurately identifying malapposed device segments across the aneurysm neck or near side-branch origins, OCT can guide clinical decisions such as postdilation or additional device deployment. Similarly, high-resolution assessment of coiling and intrasaccular device placement (including coil protrusion, neck coverage, and residual gaps) provides a more detailed characterization of procedural outcomes. Moreover, the detection of iatrogenic dissections after device deployment allows for corrective measures, and the identification of in-stent thrombus or microthrombi, often not

J NeuroIntervent Surg: first published as 10.1136/jnis-2025-024359 on 20 February 2026. Downloaded from http://jnis.bmj.com/ on November 15, 2026 by guest. Protected by copyright, including for uses related to text and data mining, AI training, and similar technologies.

visible on DSA or cone-beam CTA, can inform antiplatelet and fibrinolytic management.

At follow-up, OCT enables detailed evaluation of device endothelialization and the aneurysm healing process. The degree of neointimal coverage over metallic devices, or lack thereof, as well as early detection of neointimal hyperplasia can guide patient management. The use of OCT in clinical research may in the future assist in better understanding and optimizing of antiplatelet management strategies. Persistent aneurysm neck filling or delayed occlusion, which may indicate a risk of (re)rupture, can similarly inform the need for further treatment. In cases of late complications or suboptimal technical or clinical outcomes, high-resolution assessment of the underlying mechanisms (ie, excessive endothelialization, vasospasm, late-acquired malapposition or underexpansion across the neck, leading to delayed occlusion, or jailed branches and perforators) may potentially help, in the future, to elucidate the best re-treatment strategies to optimize long-term outcomes.

OCT applications in intracranial atherosclerotic disease

Intracranial atherosclerotic disease (ICAD) remains associated with a high risk of recurrent ischemic stroke despite optimal medical management and available interventional therapies. As with aneurysms, DSA, CTA, and MRA are the standard first-line imaging modalities for detecting and characterizing intracranial stenosis. These techniques primarily evaluate luminal narrowing and blood flow, key diagnostic parameters, but they lack the ability to characterize the morphological and structural features of ICAD. MRI vessel wall imaging offers complementary information but remains limited by a spatial resolution greater than 0.4 mm. The high-resolution, tissue-level visualization provided by OCT could have a transformative impact on the diagnosis of ICAD, as well as in its management and treatment.

Accurate quantification of the stenotic area (particularly in cases of eccentric plaque buildup) has been shown to predict ischemic risk.[6] Furthermore, detailed characterization of plaque composition (eg, fibrotic, lipid-rich, or fibrocalcific) and morphology, including parameters such as maximum lipid arc calcium distribution and thickness, as well as detection of a plaque rupture or erosion associated with thrombosis, may further refine patient selection for endovascular therapy.[33] In cases where endovascular treatment is pursued, OCT-guided evaluation can assist procedural planning, which may potentially lower the risk of recurrence and complications.

When treating lipid-rich plaques, precise device sizing (such as selecting the appropriate stent or balloon length and diameter) is essential to ensure complete lesion coverage or avoid landing device edges in an area with significant plaque, which may result in dissections or intramural hematomas. Similarly, identification of the location of plaques and perforating arteries and assessment of their state following intervention may assist in avoiding perforator-related complications. Stenosed fibrocalcific plaques can lead to suboptimal stent deployment. Neurointerventional OCT studies have linked insufficient expansion to a higher incidence of in-stent restenosis,[31] with macrocalcifications posing a greater risk of in-stent restenosis compared with small, superficial calcific deposits.[32] Consequently, detailed evaluation of intracranial calcification using OCT offers several potential advantages. It can improve patient selection for both endovascular and medical management, while in interventional cases, high-resolution calcium characterization can better guide lesion preparation strategies, such as targeted balloon angioplasty or plaque modification, to achieve acceptable expansion.

To summarize, recognition of stent malapposition or insufficient expansion allows for immediate optimization (eg, targeted balloon angioplasty), when appropriate. Precise identification and characterization of iatrogenic dissections, including their location and severity, as well as detection of intramural hematomas or residual thrombus, can guide corrective measures such as the deployment of an additional stent. Plaque severity and location of perforating arteries and characteristics of side branches (eg, ostial disease) may aid procedural strategy. In the event of mid- to long-term post-procedural complications, OCT can also provide critical insight into the underlying mechanisms of luminal restenosis or occlusion (eg, thrombosis, neoatherosclerosis, or excessive intimal proliferation), thereby informing the selection of the most effective subsequent treatment strategy. The future routine use of OCT could also facilitate the systematic collection of novel clinical data, helping to improve the current understanding of the mechanisms underlying adverse events in the treatment of intracranial stenosis.

OCT applications for acute ischemic stroke

Endovascular thrombectomy has rapidly become the standard of care for the treatment of large vessel occlusions causing acute ischemic stroke. While angiography can confirm vessel recanalization and estimate the extent of reperfusion, it provides limited information on vessel wall pathology and, following mechanical thrombectomy, the presence of residual thrombus. Post-thrombectomy, OCT can be used to identify residual thrombus adherent to the vessel wall or at the origin of jailed branches, the underlying wall pathology (eg, presence of ICAD), as well as iatrogenic complications (eg, dissections, intimal injury, or intramural hematomas). As such, the complementary information provided by OCT may help operators to determine whether an intervention can be safely concluded or if corrective actions are warranted to mitigate complications. In the case of suboptimal results, OCT assessment might further inform when a conservative approach (eg, antiplatelet therapy and monitoring) may be preferred over further mechanical intervention or stenting. The presence of ICAD and plaque characteristics that may predispose to acute re-thrombosis can be visualized, which may guide the use of stenting or other adjunctive treatments. In such cases, OCT can be of further assistance to optimize device selection (ie, by informing stent diameter, length, and placement location), potentially enhancing procedural safety and outcomes. Recent studies have shown that following microcatheter advancement distal to the thrombus and limited contrast media injection, OCT can successfully be used to image occluded vessels.[44] By enabling a detailed assessment of arterial pathologies (eg, ICAD, dissections, or vasculitis), as well as exact clot location and features (ie, size, length, and extent of erythrocyte composition), OCT may provide insights that can be used to guide the treatment strategy, especially in cases with ambiguous presentation.

A list of the potential applications discussed for hemorrhagic stroke, intracranial atherosclerotic disease, and acute ischemic stroke is provided in table 2.

FORWARD-LOOKING STATEMENT

While this article focuses primarily on vascular applications, the high-resolution extravascular imaging capabilities of the *n*OCT platform, combined with its probe design, may expand its use into additional neurointerventional domains. These capabilities could support a broader range of venous, transvascular, and intracranial procedures beyond ICAD, ischemic, and hemorrhagic stroke. Moreover, the high resolution of OCT makes it well suited for integration with machine learning-based approaches,

J NeuroIntervent Surg: first published as 10.1136/jnis-2025-024359 on 20 February 2026. Downloaded from http://jnis.bmj.com/ on November 15, 2026 by guest. Protected by copyright, including for uses related to text and data mining, AI training, and similar technologies.

Table 2 List of some of the potential applications of OCT for the characterization, management, and treatment of intracranial artery disease

Disease	Procedure	Imaging insights	Potential applications
Aneurysm	Native aneurysm assessment	► Dome tissue characteristics (eg, thickness) ► Neck anatomy and neck tissue characteristics ► Presence of clots ► Presence of erythrocytes in the CSF ► Parent artery size ► Vessel wall disease in the parent artery	► Assess aneurysm risk of clinical events ► Guide device selection and sizing ► Inform optimal device placement location
	Acute treatment assessment	Stent and flow diverters ► Assess device coverage over the aneurysm neck ► Assess device apposition and expansion ► Assess acute thrombus formation Coils and intrasaccular devices ► Neck coverage and presence of gaps ► Device protrusion into the parent artery	► Inform corrective actions (eg, angioplasty, medications, or need for additional devices)
	Follow-up assessment	► Device endothelialization and intimal hyperplasia ► Late acquired device malapposition and underexpansion ► Stenosis characteristics ► Vasospasm	► Inform patient management
	Complications	► Assess mechanisms leading to complications (eg, incomplete neck coverage, thrombosis, and late acquired malapposition)	► Inform need for re-treatment and optimal planning
ICAD	Plaque assessment	► Stenosis severity ► Plaque components and plaque size ► Plaque rupture and erosion ► Presence of thrombus ► High-risk plaque features ► Longitudinal extent of the disease ► Quantitative lumen and vessel sizing	► Assess plaque risks of clinical events and inform medical treatment vs endovascular therapy ► Identify culprit lesion in cases of multiple stenoses ► Assess need for plaque modification before stenting (eg, balloon angioplasty) ► Guide treatment, informing device selection and sizing
	Acute treatment assessment	► Stent malapposition ► Lumen expansion ► Acute or residual thrombus ► Intramural hematoma ► Assessment of dissections	► Actionable information to correct device placement (angioplasty) ► Assess need for additional treatment
	Follow-up assessment	► Stent endothelialization ► Side-branch patency ► Early detection of subclinical restenosis	► Guide medical therapy
	Complications	► Assess stent thrombosis and restenosis ► Elucidate mechanisms of stent failure (eg, late acquired stent malapposition, underexpansion, neointimal hyperplasia, or neoatherosclerosis) ► Vasospasm	► Inform optimal re-treatment strategy
Ischemic stroke	Native assessment of vessel occlusion	► Assess underlying artery pathology (eg, ICAD, vasculitis, and dissection) ► Assess clot location, size, and composition	► Inform treatment decisions (eg, thrombus mechanical removal and stenting) ► Device sizing and placement location
	Acute treatment assessment	► Iatrogenic dissection ► Residual thrombus ► Side branches and perforating arteries patency ► Intramural hematoma	► Inform corrective actions (further clot removal attempts, anti-thrombotic medications, or device placement)
	Complications	► Mechanism leading to reocclusion (eg, underlying ICAD and dissection)	► Inform optimal re-treatment decision

CSF, cerebrospinal fluid; ICAD, intracranial atherosclerotic disease.

which could automate the image analysis workflow, facilitating and accelerating clinical adoption. The future incorporation of software-based angiographic co-registration may further facilitate use of OCT as a complementary modality alongside angiographic techniques. Furthermore, OCT may also find a future role in providing periprocedural guidance in robotic-assisted neurovascular interventions.[68]

Supported by extensive evidence from cardiovascular and peripheral applications, this article aimed to establish a foundation for interpreting and analyzing OCT images within intracranial artery disease and to aid its clinical translation into neurointerventional practice. A neuro-dedicated OCT device has the potential not only to become a routine diagnostic tool in neurointervention but, by enabling visualization of devices and tissue characteristics at a higher resolution, it may also become a key technology in neurovascular research, supporting detailed in vivo evaluation of novel therapies and treatments for neurointervention.

It is important to acknowledge that the evidence supporting the use of OCT in neurointerventional surgery remains at an early stage. Although initial studies showed promising safety and effectiveness data, the available data are limited by small sample

J NeuroIntervent Surg: first published as 10.1136/jnis-2025-024359 on 20 February 2026. Downloaded from http://jnis.bmj.com/ on November 15, 2026 by guest. Protected by copyright, including for uses related to text and data mining, AI training, and similar technologies.

sizes. While OCT has been extensively validated for vascular imaging, further studies are needed to evaluate its imaging capabilities for specific neurovascular conditions in comparison with vessel histopathology. Preclinical investigations have demonstrated that OCT can complement and enhance diagnoses obtained using DSA and cone-beam CT alone[9]; however, future clinical studies are required to establish the extent to which OCT can add value alongside these modalities in routine practice. Future clinical research should also focus on identifying and optimizing strategies for the application of OCT in neurointerventional procedures. The impact of OCT on procedural duration, contrast utilization, and X-ray radiation exposure in real-world clinical settings remains unknown. Experience from cardiovascular applications suggests that systematic OCT workflows may reduce X-ray radiation without increasing contrast use,[22] but this hypothesis requires re-validation in neurointerventional contexts. Furthermore, as with every new image modality, image interpretation will have a learning curve for new users. The development of standardized clinical OCT imaging workflows can help to minimize this learning curve and enable efficient integration into clinical practice, but this remains another area for future investigation. Similarly, robust outcome data and cost-effectiveness analyses assessing the impact of OCT on clinical practice will be the focus of future studies.

CONCLUSION

Intravascular OCT is a high-resolution imaging modality that is expanding from coronary to cerebrovascular applications. Building on decades of evidence from cardiovascular and peripheral use, clinicians will soon be able to perform routine 'optical histology' of intracranial arteries and implanted devices using neuro-dedicated OCT technology. This article may serve as a reference for researchers and clinicians for the interpretation and analysis of neurovascular OCT images.

MATERIAL AND METHODS

Search strategy and selection criteria

References for the use of OCT in coronary arteries were derived by a Medline (PubMed) search using the following query:

- (((optical coherence tomography) OR (intravascular imaging)) AND (coronary) AND ((meta-analysis (filter) OR randomized controlled trial (filter)) AND (English (filter)) AND (all adult((filter)) AND (2020:2025 (pdat)))) AND ((meta-analysis (filter) OR randomized controlled trial(-filter)) AND (English (filter)) AND (all adult (filter))).

References for the use of OCT in neurointervention were derived by a Medline (PubMed) search using the following query:

- ((optical coherence tomography) AND ((intravascular) OR (endovascular))) AND ((intracranial) OR (neurovascular) OR (cerebrovascular) OR (internal carotid) OR (basilar) OR (vertebral)) NOT (review (publication type)).

References for the use of OCT in coronary arteries and in neurointervention were also supplemented by a database maintained by the authors. References for OCT technology were derived from a database maintained by the authors and, throughout the manuscript, to further restrict the number of references cited, priorities were given to original observations, randomized trials, and multicenter studies, when possible.

Author affiliations
[1]Department of Neurosurgery, Advocate Lutheran General Hospital, Park Ridge, Illinois, USA
[2]Department of Cerebrovascular Surgery, Baptist Neurological Institute, Lyerly Neurosurgery, Jacksonville, Florida, USA
[3]New England Center for Stroke Research, University of Massachusetts Chan Medical School, Worcester, Massachusetts, USA
[4]Department of Neurosurgery, St Michael's Hospital, Toronto, Ontario, Canada
[5]University Medical Center Hamburg-Eppendorf, Hamburg, Germany
[6]Eppdata GmbH, Hamburg, Germany
[7]Department of Interventional Neuroradiology, Clinica La Sagrada Familia, Buenos Aires, Argentina
[8]Department of Interventional Neuroradiology, Centre Hospitalier Universitaire de Limoges, Limoges, France
[9]CHU Limoges, Limoges, Aquitaine-Limousin-Poitou-Charentes, France
[10]Department of Neuroradiology, Clermont Hospital Center, Clermont, Hauts-de-France, France
[11]St Michael's Hospital, Toronto, Ontario, Canada
[12]Department of Neurosurgery, Tufts Medical Center, Boston, Massachusetts, USA
[13]Department of Neurosurgery, University of South Florida, Tampa, Florida, USA
[14]Department of Neurosurgery, BIDMC, Boston, Massachusetts, USA
[15]Cardiovascular Division, Beth Israel Deaconess Medical Center, Boston, Massachusetts, USA
[16]Harvard Medical School, Boston, Massachusetts, USA
[17]Department of Interventional Cardiology, Tampa General Hospital, Tampa, Florida, USA
[18]Kawasaki Medical School, Kurashiki, Okayama Prefecture, Japan
[19]University at Buffalo Neurosurgery Inc, Buffalo, New York, USA
[20]Department of Neuroradiology, Karolinska University Hospital, Stockholm, Sweden
[21]Department of Clinical Neuroscience, Karolinska Institutet, Stockholm, Sweden
[22]New England Center for Stroke Research, Department of Radiology, University of Massachusetts Chan Medical School, Worcester, Massachusetts, USA
[23]Department of Radiology, University of Massachusetts Medical School, Worcester, Massachusetts, USA
[24]Advanced Development, Spryte Medical, Bedford, Massachusetts, USA

Contributors Drafting of the manuscript, figures, and conceptualization: TA, MJG, and GJU. Critical revision of the manuscript and figures: all authors. Writing editing: all authors.

Funding The authors have not declared a specific grant for this research from any funding agency in the public, commercial or not-for-profit sectors.

Competing interests VA and TA received consulting fees from Spryte Medical. MJG received honoraria for lectures and presentations and is PI on contracts from Spryte Medical to UMASS Chan Medical School. DL, RAH, VA, NMC, TA, PL, VMP, and MJG received ad hoc travel support from Spryte Medical. VMP, DL, and MJG participated in ad hoc Advisory Board meetings for Spryte Medical. GJU is an employee of Spryte Medical.

Patient consent for publication Not applicable.

Ethics approval Not applicable.

Provenance and peer review Commissioned; externally peer reviewed.

Supplemental material This content has been supplied by the author(s). It has not been vetted by BMJ Publishing Group Limited (BMJ) and may not have been peer-reviewed. Any opinions or recommendations discussed are solely those of the author(s) and are not endorsed by BMJ. BMJ disclaims all liability and responsibility arising from any reliance placed on the content. Where the content includes any translated material, BMJ does not warrant the accuracy and reliability of the translations (including but not limited to local regulations, clinical guidelines, terminology, drug names and drug dosages), and is not responsible for any error and/or omissions arising from translation and adaptation or otherwise.

ORCID iDs
Vania Anagnostakou https://orcid.org/0000-0001-5101-3192
Nicole M Cancelliere https://orcid.org/0000-0002-8703-4304
Ivan Lylyk https://orcid.org/0000-0002-6048-4225
Aymeric Rouchaud https://orcid.org/0000-0003-0902-3375
Géraud Forestier https://orcid.org/0000-0003-4797-9693
Adel M Malek https://orcid.org/0000-0002-0642-7609
Kunal Vakharia https://orcid.org/0000-0001-8222-8874
Christopher S Ogilvy https://orcid.org/0000-0003-4600-8545
Matthew J Gounis https://orcid.org/0000-0002-8034-2785
Giovanni J Ughi https://orcid.org/0000-0003-3354-0698

REFERENCES

1 Araki M, Park S-J, Dauerman HL, *et al*. Optical coherence tomography in coronary atherosclerosis assessment and intervention. *Nat Rev Cardiol* 2022;19:684–703.

J NeuroIntervent Surg: first published as 10.1136/jnis-2025-024359 on 20 February 2026. Downloaded from http://jnis.bmj.com/ on November 15, 2026 by guest. Protected by copyright, including for uses related to text and data mining, AI training, and similar technologies.

2 Kang D-Y, Ahn J-M, Yun S-C, *et al*. Optical Coherence Tomography-Guided or Intravascular Ultrasound-Guided Percutaneous Coronary Intervention: The OCTIVUS Randomized Clinical Trial. *Circulation* 2023;148:1195–206.
3 Maehara A, Mintz GS, Stone GW. OCT versus IVUS: accuracy versus clinical utility. *JACC Cardiovasc Imaging* 2013;6:1105–7.
4 Gerbaud E, Weisz G, Tanaka A, *et al*. Multi-laboratory inter-institute reproducibility study of IVOCT and IVUS assessments using published consensus document definitions. *Eur Heart J Cardiovasc Imaging* 2016;17:756–64.
5 Swanson EA, Fujimoto JG. The ecosystem that powered the translation of OCT from fundamental research to clinical and commercial impact. *Biomed Opt Express* 2017;8:1638–64.
6 Feng Y, Wu T, Wang T, *et al*. Correlation between intracranial vertebral artery stenosis diameter measured by digital subtraction angiography and cross-sectional area measured by optical coherence tomography. *J Neurointerv Surg* 2021;13:1002–6.
7 Yang B, Feng Y, Ma Y, *et al*. Frequency-Domain Optical Coherence Tomography for Intracranial Atherosclerotic Stenosis: Feasibility, Safety, and Preliminary Experience. *Front Neurol* 2021;12:678443.
8 Gounis MJ, Ughi GJ, Marosfoi M, *et al*. Intravascular Optical Coherence Tomography for Neurointerventional Surgery. *Stroke* 2019;50:218–23.
9 Ughi GJ, Marosfoi MG, King RM, *et al*. A neurovascular high-frequency optical coherence tomography system enables in situ cerebrovascular volumetric microscopy. *Nat Commun* 2020;11:3851.
10 Tang T, Zhou J, Thomas AM, *et al*. A systematic review of application of frequency-domain optical coherence tomography in cerebral large artery atherosclerosis. *Neuroradiology* 2025;67:1139–51.
11 Karavolias I, Roy JM, Musmar B, *et al*. Optical coherence tomography in endovascular neurosurgery: current applications and future directions. *J Clin Neurosci* 2025;141:111563.
12 Yun SH, Tearney GJ, Vakoc BJ, *et al*. Comprehensive volumetric optical microscopy in vivo. *Nat Med* 2006;12:1429–33.
13 Bezerra HG, Costa MA, Guagliumi G, *et al*. Intracoronary optical coherence tomography: a comprehensive review clinical and research applications. *JACC Cardiovasc Interv* 2009;2:1035–46.
14 Bezerra HG, Quimby DL, Matar F, *et al*. High-Frequency Optical Coherence Tomography (HF-OCT) for Preintervention Coronary Imaging: A First-in-Human Study. *JACC Cardiovasc Imaging* 2023;16:982–4.
15 Quimby DL Jr, Rothstein ES, Richmond HCT, *et al*. Efficacy and Safety of High-Frequency Optical Coherence Tomography (HF-OCT) for Coronary Imaging: A Multicenter Study. *J Soc Cardiovasc Angiogr Interv* 2025;4:102577.
16 Shlofmitz E, Croce K, Bezerra H, *et al*. The MLD MAX OCT algorithm: An imaging-based workflow for percutaneous coronary intervention. *Cathet Cardio Intervent* 2022;100:S7–13.
17 Riley RF, Patel MP, Abbott JD, *et al*. SCAI Expert Consensus Statement on the Management of Calcified Coronary Lesions. *Journal of the Society for Cardiovascular Angiography & Interventions* 2024;3:101259.
18 Onuma Y, Katagiri Y, Burzotta F, *et al*. Joint consensus on the use of OCT in coronary bifurcation lesions by the European and Japanese bifurcation clubs. *EuroIntervention* 2019;14:e1568–77.
19 Erdogan E, Bajaj R, Lansky A, *et al*. Intravascular Imaging for Guiding In-Stent Restenosis and Stent Thrombosis Therapy. *J Am Heart Assoc* 2022;11:e026492.
20 van der Sijde JN, Karanasos A, van Ditzhuijzen NS, *et al*. Safety of optical coherence tomography in daily practice: a comparison with intravascular ultrasound. *Eur Heart J Cardiovasc Imaging* 2017;18:467–74.
21 Hong S-J, Lee S-J, Lee S-H, *et al*. Optical coherence tomography-guided versus angiography-guided percutaneous coronary intervention for patients with complex lesions (OCCUPI): an investigator-initiated, multicentre, randomised, open-label, superiority trial in South Korea. *Lancet* 2024;404:1029–39.
22 Osborn EA, Johnson M, Maksoud A, *et al*. Safety and efficiency of percutaneous coronary intervention using a standardised optical coherence tomography workflow. *EuroIntervention* 2023;18:1178–87.
23 Lee JM, Choi KH, Song YB, *et al*. Intravascular Imaging-Guided or Angiography-Guided Complex PCI. *N Engl J Med* 2023;388:1668–79.
24 Ali ZA, Landmesser U, Maehara A, *et al*. Optical Coherence Tomography-Guided versus Angiography-Guided PCI. *N Engl J Med* 2023;389:1466–76.
25 Holm NR, Andreasen LN, Neghabat O, *et al*. OCT or Angiography Guidance for PCI in Complex Bifurcation Lesions. *N Engl J Med* 2023;389:1477–87.
26 Stone GW, Christiansen EH, Ali ZA, *et al*. Intravascular imaging-guided coronary drug-eluting stent implantation: an updated network meta-analysis. *The Lancet* 2024;403:824–37.
27 Kuno T, Kiyohara Y, Maehara A, *et al*. Comparison of Intravascular Imaging, Functional, or Angiographically Guided Coronary Intervention. *J Am Coll Cardiol* 2023;82:2167–76.
28 Rao SV, O'Donoghue ML, Ruel M, *et al*. 2025 ACC/AHA/ACEP/NAEMSP/SCAI Guideline for the Management of Patients With Acute Coronary Syndromes: A Report of the American College of Cardiology/American Heart Association Joint Committee on Clinical Practice Guidelines. *Circulation* 2025;151:e771–862.
29 Vrints C, Andreotti F, Koskinas KC, *et al*. 2024 ESC Guidelines for the management of chronic coronary syndromes. *Eur Heart J* 2024;45:3415–537.
30 Ozaki Y, Tobe A, Onuma Y, *et al*. CVIT expert consensus document on primary percutaneous coronary intervention (PCI) for acute coronary syndromes (ACS) in 2024. *Cardiovasc Interv Ther* 2024;39:335–75.
31 Xu R, Yang B, Li L, *et al*. Macrocalcification of intracranial vertebral artery may be related to in-stent restenosis: lessons learned from optical coherence tomography. *J Neurointerv Surg* 2022;14.
32 Li T, Xu R, Ma Y, *et al*. Calcification is a risk factor for intracranial in-stent restenosis: an optical coherence tomography study. *J NeuroIntervent Surg* 2024;16:897–901.
33 Xu R, Yang B, Wang T, *et al*. Prevalence of intracerebral thrombus detected by optical coherence tomography in patients with posterior circulation stroke or transient ischemic attack. *J NeuroIntervent Surg* 2025;17:1045–50.
34 Gutiérrez-Baños J de J, Castillo-Rangel C, Rodriguez-Pereira MI, *et al*. Early experience using optical coherence tomography for intraluminal evaluation of vascular healing associated with endovascular treatment of intracranial aneurysms. *J Neurosurg* 2025;143:668–77.
35 Martínez-Galdámez M, Escartín J, Pabón B, *et al*. Optical coherence tomography: Translation from 3D-printed vascular models of the anterior cerebral circulation to the first human images of implanted surface modified flow diverters. *Interv Neuroradiol* 2019;25:150–6.
36 Su J, Mathews M, Nwagwu C, *et al*. *Imaging Treated Brain Aneurysms in Vivo Using Optical Coherence.* tomography: SPIE, 2008.
37 Mathews MS, Su J, Heidari E, *et al*. Neuroendovascular optical coherence tomography imaging and histological analysis. *Neurosurgery* 2011;69:430–9.
38 King RM, Peker A, Epshtein M, *et al*. Active drug-coated flow diverter in a preclinical model of intracranial stenting. *J NeuroIntervent Surg* 2024;16:731–6.
39 Anagnostakou V, Epshtein M, Ughi GJ, *et al*. Transvascular in vivo microscopy of the subarachnoid space. *J Neurointerv Surg* 2022;14:420–8.
40 Vardar Z, King RM, Kraitem A, *et al*. High-resolution image-guided WEB aneurysm embolization by high-frequency optical coherence tomography. *J Neurointerv Surg* 2021;13:669–73.
41 King RM, Langan ET, Ughi GJ, *et al*. Acute Thrombus Burden on Coated Flow Diverters Assessed by High Frequency Optical Coherence Tomography. *Cardiovasc Intervent Radiol* 2020;43:1218–23.
42 Caroff J, King RM, Ughi GJ, *et al*. Longitudinal Monitoring of Flow-Diverting Stent Tissue Coverage After Implant in a Bifurcation Model Using Neurovascular High-Frequency Optical Coherence Tomography. *Neurosurgery* 2020;87:1311–9.
43 King RM, Marosfoi M, Caroff J, *et al*. High frequency optical coherence tomography assessment of homogenous neck coverage by intrasaccular devices predicts successful aneurysm occlusion. *J Neurointerv Surg* 2019;11:1150–4.
44 Pereira VM, Lylyk P, Cancelliere N, *et al*. Volumetric microscopy of cerebral arteries with a miniaturized optical coherence tomography imaging probe. *Sci Transl Med* 2024;16:eadl4497.
45 van Soest G, Goderie T, Regar E, *et al*. Atherosclerotic tissue characterization in vivo by optical coherence tomography attenuation imaging. *J Biomed Opt* 2010;15:011105.
46 Tearney GJ, Yabushita H, Houser SL, *et al*. Quantification of macrophage content in atherosclerotic plaques by optical coherence tomography. *Circulation* 2003;107:113–9.
47 Yabushita H, Bouma BE, Houser SL, *et al*. Characterization of Human Atherosclerosis by Optical Coherence Tomography. *Circulation* 2002;106:1640–5.
48 Xu C, Schmitt JM, Carlier SG, *et al*. Characterization of atherosclerosis plaques by measuring both backscattering and attenuation coefficients in optical coherence tomography. *J Biomed Opt* 2008;13:034003.
49 Malle C, Tada T, Steigerwald K, *et al*. Tissue Characterization After Drug-Eluting Stent Implantation Using Optical Coherence Tomography. *ATVB* 2013;33:1376–83.
50 Vuong B, Sun C, Kiehl T-R, *et al*. Feasibility and methodology of optical coherence tomography imaging of human intracranial aneurysms: ex vivo pilot study. SPIE; 2012.
51 Anagnostakou V, Epshtein M, Peker A, *et al*. New frontiers in intracranial imaging with HF-OCT: Ex vivo human cerebrovasculature evaluation and in vivo intracranial arteries dynamic visualization. *Front Photon* 2022;3.
52 King RM, Peker A, Anagnostakou V, *et al*. High-frequency optical coherence tomography predictors of aneurysm occlusion following flow diverter treatment in a preclinical model. *J Neurointerv Surg* 2023;15:919–23.
53 King RM, Brooks OW, Langan ET, *et al*. Communicating malapposition of flow diverters assessed with optical coherence tomography correlates with delayed aneurysm occlusion. *J Neurointerv Surg* 2018;10:693–7.
54 Pasarikovski CR, Ku JC, Ramjist J, *et al*. Minimally invasive intrathecal spinal cord imaging with optical coherence tomography. *J Biomed Opt* 2021;26:056002.
55 Anagnostakou V, Ughi GJ, King R, *et al*. Endoscopic optical coherence tomography imaging: Practical applications for intracranial aneurysms. *Journal of Neurointervention* 2025.
56 Tearney GJ, Regar E, Akasaka T, *et al*. Consensus standards for acquisition, measurement, and reporting of intravascular optical coherence tomography studies: a report from the International Working Group for Intravascular Optical Coherence Tomography Standardization and Validation. *J Am Coll Cardiol* 2012;59:1058–72.
57 Durand E, Scoazec A, Lafont A, *et al*. In vivo induction of endothelial apoptosis leads to vessel thrombosis and endothelial denudation: a clue to the understanding of the mechanisms of thrombotic plaque erosion. *Circulation* 2004;109:2503–6.

J NeuroIntervent Surg: first published as 10.1136/jnis-2025-024359 on 20 February 2026. Downloaded from http://jnis.bmj.com/ on November 15, 2026 by guest. Protected by copyright, including for uses related to text and data mining, AI training, and similar technologies.

58 Fahed AC, Jang IK. Plaque erosion and acute coronary syndromes: phenotype, molecular characteristics and future directions. *Nat Rev Cardiol* 2021;18:724–34.
59 Torii S, Sato Y, Otsuka F, *et al*. Eruptive Calcified Nodules as a Potential Mechanism of Acute Coronary Thrombosis and Sudden Death. *J Am Coll Cardiol* 2021;77:1599–611.
60 Moreno PR, Purushothaman KR, Fuster V, *et al*. Plaque neovascularization is increased in ruptured atherosclerotic lesions of human aorta: implications for plaque vulnerability. *Circulation* 2004;110:2032–8.
61 Nishi T, Kume T, Yamada R, *et al*. Variation of the Appearance of Intraplaque Hemorrhage on Optical Coherence Tomography and Intravascular Ultrasound. *JACC: Cardiovascular Interventions* 2023;16:997–9.
62 Zoppo CT, Kolstad JW, King RM, *et al*. A novel intrasaccular aneurysm device with high complete occlusion rate: initial results in a rabbit model. *J NeuroIntervent Surg* 2024;16:928–33.
63 Morel S, Diagbouga MR, Dupuy N, *et al*. Correlating Clinical Risk Factors and Histological Features in Ruptured and Unruptured Human Intracranial Aneurysms: The Swiss AneuX Study. *J Neuropathol Exp Neurol* 2018;77:555–66.
64 Frösen J, Piippo A, Paetau A, *et al*. Remodeling of saccular cerebral artery aneurysm wall is associated with rupture: histological analysis of 24 unruptured and 42 ruptured cases. *Stroke* 2004;35:2287–93.
65 Suzuki J, Ohara H. Clinicopathological study of cerebral aneurysms. Origin, rupture, repair, and growth. *J Neurosurg* 1978;48:505–14.
66 Ishii D, Nakagawa D, Zanaty M, *et al*. Quantitative Susceptibility Mapping and Vessel Wall Imaging as Screening Tools to Detect Microbleed in Sentinel Headache. *J Clin Med* 2020;9:979.
67 Rouchaud A, Ramana C, Brinjikji W, *et al*. Wall Apposition Is a Key Factor for Aneurysm Occlusion after Flow Diversion: A Histologic Evaluation in 41 Rabbits. *AJNR Am J Neuroradiol* 2016;37:2087–91.
68 Mendes Pereira V, Cancelliere NM, Nicholson P, *et al*. First-in-human, robotic-assisted neuroendovascular intervention. *J Neurointerv Surg* 2020;12:338–40.
69 Patel IJ, Bezerra HG, Costa MA, *et al*. Novel use of optical coherence tomography. *J Neurointerv Surg* 2013;5:e41.
70 Brouwer P, Ligthart J, Regar E. P-010 Optical Coherence Tomography (OCT) Before and After Flowdiverter Treatment in Basilar Dolichoectasia. *J NeuroIntervent Surg* 2014;6:A25.
71 Given CA II, Ramsey CN III, Attizzani GF, *et al*. Optical coherence tomography of the intracranial vasculature and Wingspan stent in a patient. *BMJ Case Rep* 2014.
72 Griessenauer CJ, Gupta R, Shi S, *et al*. Collar Sign in Incompletely Occluded Aneurysms after Pipeline Embolization: Evaluation with Angiography and Optical Coherence Tomography. *AJNR Am J Neuroradiol* 2017;38:323–6.
73 Gao P, Gui L, Yang B, *et al*. Optical Coherence Tomography of Spontaneous Basilar Artery Dissection in a Patient With Acute Ischemic Stroke. *Front Neurol* 2018;9:858.
74 Pasarikovski CR, Ramjist J, da Costa L, *et al*. Optical coherence tomography imaging after endovascular thrombectomy for basilar artery occlusion: report of 3 cases. *J Neurosurg* 2019;133:1141–6.
75 Li L, Dmytriw AA, Krings T, *et al*. Visualization of the Human Intracranial Vasa Vasorum In Vivo Using Optical Coherence Tomography. *JAMA Neurol* 2020;77:903.
76 Xu X, Li M, Liu R, *et al*. Optical coherence tomography evaluation of vertebrobasilar artery stenosis: case series and literature review. *J Neurointerv Surg* 2020;12:809–13.
77 Feng Y, Dmytriw AA, Yang B, *et al*. Neovascularization in Human Intracranial Atherosclerotic In-Stent Restenosis. *Diagnostics (Basel)* 2021;11:322.
78 Neira RI, Yamada K, Shirakawa M, *et al*. Application of Optical Frequency Domain Imaging to Recanalized Unruptured Internal Carotid Artery Aneurysm Treated by Flow-Diverting Stent-Assisted Coiling. *World Neurosurg* 2021;146:1–5.
79 Li D, Tang T, Hu T, *et al*. Teaching NeuroImage: Etiologic Investigation Using Optical Coherence Tomography During Thrombectomy. *Neurology (ECronicon)* 2023;101:280–1.
80 Li D, Tang T, Hu T, *et al*. Application of optical coherence tomography in decision-making of post-thrombectomy adjunctive treatments. *J Neurointerv Surg* 2023;15:616–8.
81 Li D, Tang T, Hu T, *et al*. Utilization of Optical Coherence Tomography in the Diagnosis of Intraplaque Hemorrhage Causing Severe Basilar Artery Stenosis. *Stroke* 2024;55:e132–3.
82 Ma Y, Ji Z, Yang W, *et al*. Role of optical coherence tomography in pipeline embolization device for the treatment of vertebral–basilar artery dissecting aneurysms. *J NeuroIntervent Surg* 2024;16:308–12.

J NeuroIntervent Surg: first published as 10.1136/jnis-2025-024359 on 20 February 2026. Downloaded from http://jnis.bmj.com/ on November 15, 2026 by guest. Protected by copyright, including for uses related to text and data mining, AI training, and similar technologies.